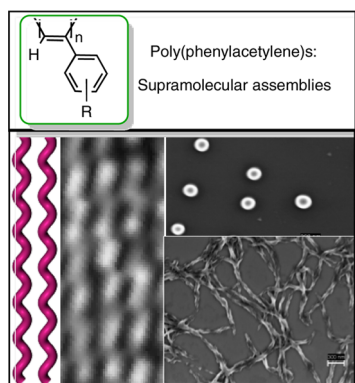# Supramolecular Assemblies from Poly(phenylacetylene)s

Félix Freire, Emilio Quiñoá, and Ricardo Riguera*

Department of Organic Chemistry and Center for Research in Biological Chemistry and Molecular Materials (CIQUS), University of Santiago de Compostela, E-15782 Santiago de Compostela, Spain

Poly(phenylacetylene)s:
Supramolecular assemblies

CONTENTS

1. INTRODUCTION

The evolution of chemistry in the last 60 years can be illustrated by the introduction of just a few new concepts. One is *macromolecules*,[1,2] whose importance was recognized in the 1953 Nobel Prize to Prof. Staudinger, and the other two are *molecular recognition* and *supramolecular assembly*,[3−5] which gave the 1987 Nobel Prize to Profs. Cram, Lehn, and Pedersen.

Supramolecular assemblies may present different architectures (films, layers, membranes, spheres, etc.) depending on the type of bonding that binds the molecular components together and how they are spatially arranged. If the components are chiral, the transference of their absolute configuration to the assembly and the presence of supramolecular chirality constitute an especially appealing topic.[6−14]

Those fields of knowledge not only have covered a very important part of chemical research, industry, and academics but also have paved the way to the upsurge of nanochemistry, nanodevices, nanosensors, etc., and their applications to medicine (treatment and diagnosis), optics, magnetics, etc., aspects that are well-covered in numerous reviews and books.[15−24]

This review is dedicated to the different supramolecular assemblies that have been obtained from poly-(phenylacetylene)s (PPAs), and the reader may well be interested in knowing the reason for concentrating on this particular class of polymers as a source of supramolecular aggregates.[25−30] Phenylacetylenes have attracted the attention of researchers since the early days of polymer chemistry because they were perfect candidates to make long conjugated polyene chains whose electron-richness could be modulated by the introduction of substituents on the phenyl ring. Interestingly enough, it was the observation that in many PPAs the polyene chain adopts a nonflat helical structure that opened the field to other perspectives associated with their helicity.[31]

Hence, PPA polymers and copolymers with more or less marked helicity or planarity and with a variety of functional groups can be prepared, where a planar extended polyene conjugated system is the key point or, on the contrary, where the plus is given by their chirality, represented by a preferred *P* or *M* helical sense.

The helical backbone is not rigid but rather is dynamic, where the presence of an external stimulus can affect not only the helical sense induced in the helical polymer[32−36] but also the stretching or compression of the helical scaffold.[32,37−43] Thus, chiral amplification toward a specific helical sense or helical inversion between the *P* and *M* helices can be accompanied by elongation or compression of the helical structure.

In these polymers, the helicity of the backbone is transmitted to the pendants (e.g., the phenyl ring in PPA), which constitute the external part of the polymer. The pendants also describe a helical structure showing more or less elongated helices with the same or opposite sense than the helix described by the polyene backbone.[32,36] Naturally, the distances and spatial relationship between the pendants are different depending on the helical structure adopted by the polymer. While circular
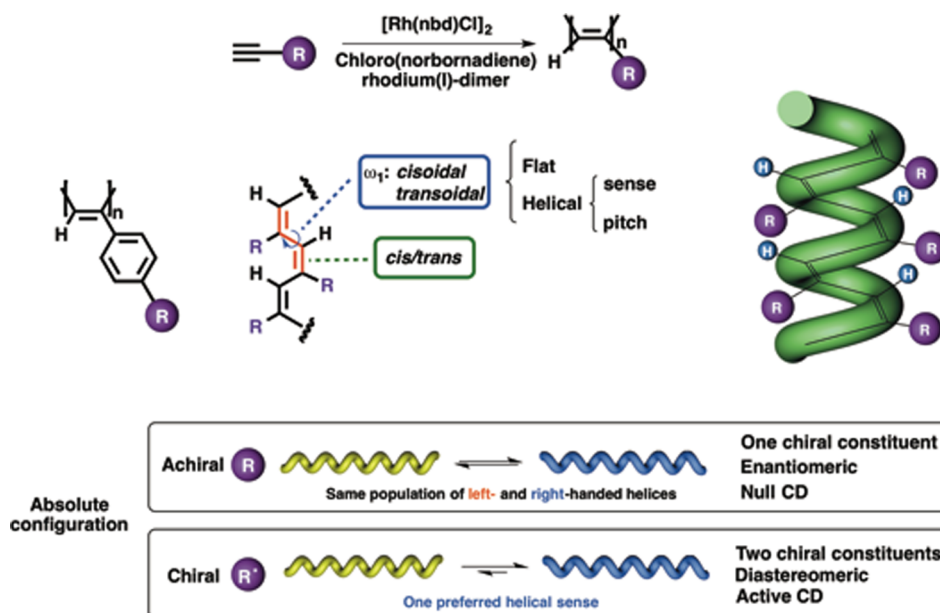
Figure 1. Structure of poly(phenylacetylene)s: configuration and conformation.
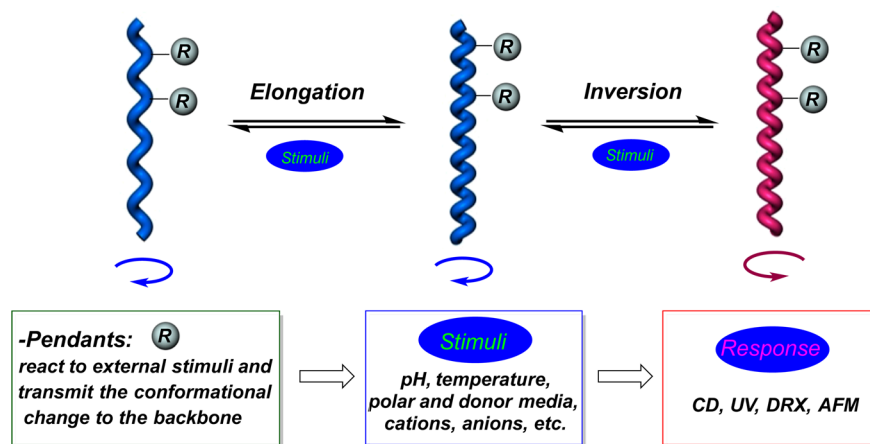

Figure 2. Schematic representation of the different effects on the structure of a dynamic helical polymer produced by the action of external stimuli.

dichroism (CD) measurements can easily examine the internal helicity of the polymer backbone, the external helix is usually visualized by atomic force microscopy (AFM) and related techniques.

The presence in the pendants of substituents with supramolecular binding abilities, e.g., long alkyl chains, explains the conversion of PPAs into a variety of supramolecular assemblies that reflect the helical structure of the starting polymer. Thus, good knowledge of the structural characteristics, configuration, and conformation of the PPAs is crucial for understanding the resulting supramolecular aggregates, which can be macroscopically chiral thanks to the helical structure of the polymers.

In this review, we describe the state of the art around the supramolecular assemblies obtained from poly-(phenylacetylene)s. Its content is organized according to the type of aggregate [fibers, superhelices, belts, nanoparticles, nanotubes, gels, two-dimensional (2D) and oriented liquid crystals and films, and composites], preceded by an introductory section on the stereostructural characteristics that make PPAs a unique class of polymers.

2. THE STRUCTURE OF POLY(PHENYLACETYLENE)S: CONFIGURATION AND CONFORMATION

Polymerization of monosubstituted acetylenes produces conjugated polyenes with structures that depend on the catalysts used and are defined by a backbone with a cis or trans configuration of the double bonds and a cisoidal or transoidal conformation around the $C(sp^2)-C(sp^2)$ σ bonds (Figure 1). Thus, while the trans polymers (cisoidal or transoidal, respectively) have a flat structure, the polyacetylenes having cis double bonds prefer to adopt a less congested (i.e., nonflat) helix where the $C(sp^2)-C(sp^2)$ σ dihedral angle ω_1 (Figure 1) takes values (different from 0° or 180°) that determine the sense and pitch of the helix. Polymerization of phenylacetylene with a Rh(I) catalyst is a very effective way to prepare poly(phenylacetylene) with a cis configuration of the double bonds.[44−49]

The two helical senses in poly(phenylacetylene), P and M, have an enantiomeric relationship. As the energy barrier for rotation around the σ bond is low, they coexist in a 1:1 equilibrium in solution, behaving as an axially racemic polymer (null CD). Naturally, however, if a chiral group is present, e.g.,
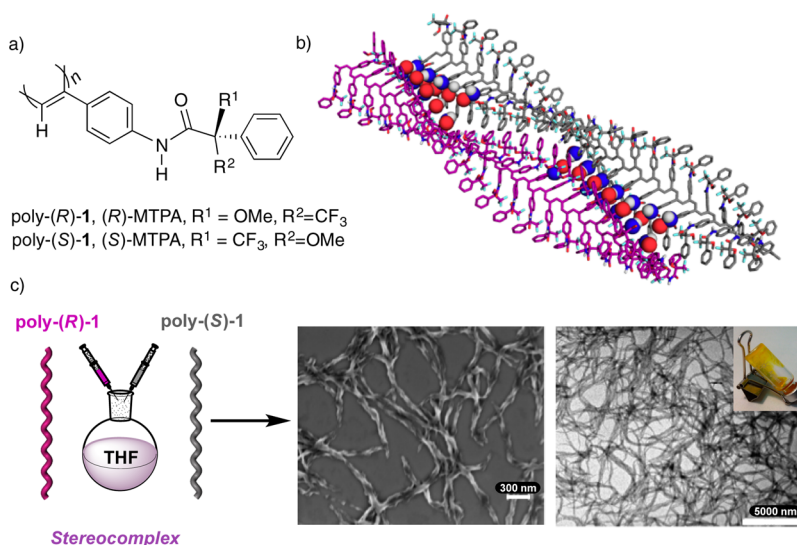
Figure 3. (a) Structures of poly-(*R*)-**1** and poly-(*S*)-**1**. (b) Simplified structural model showing the matching hydrogen bonds just between two complementary enantiomeric helices [i.e., poly-(*R*)- and poly-(*S*)-**1**]. (c) Scanning electron microscopy (SEM) images showing the fiberlike and gel structures of the stereocomplex. Adapted from ref 54, published by The Royal Society of Chemistry.

in the R substituent of the phenyl ring (Figure 1), the two helical senses of the R*-substituted poly(phenylacetylene) are no longer enantiomers. Instead, they are diastereomers, and the polymer can present a preferred *P* or *M* helical sense in the equilibrium. Therefore, a predominant helical sense is available from the *R* enantiomer, while the opposite sense can be obtained from the *S* enantiomer.[25−30] Still, the two helical senses of a PPA containing a chiral R* can be interconverted if the conformational barrier for rotation around conjugated double bonds is surpassed by manipulation of the equilibrium (e.g., with temperature), allowing the preparation of polymers whose helical sense responds to temperature changes.

Interestingly, if a polymer devoid of chirality at R* (1:1 *P/M* mixture, null CD) has functional groups that can interact with small chiral molecules, its interactions with the *R* and *S* enantiomers will yield diastereomeric complexes that should present a preferred helical sense. For instance, a poly-(phenylacetylene) carrying carboxylic acid groups in the pendants can be forced to adopt one or the other helical sense by addition of the *R* or *S* enantiomer of a chiral amine.[50−53] Acidification of the solution will cleave the salt and make the polymer lose the helical preference, opening the way to the design of helical polymers whose helicity responds to the pH.

Many other examples showing control of the helical sense and/or elongation or compression of the polymer by the action of an external stimulus such as a change in the polarity, donor character, or solvation ability of the solvent or complexation with metal ions have been described.[32,37−43] In all of those cases, the change in the helical backbone is triggered by conformational changes of the pendants, which modify the intramolecular interactions among vicinal pendants and force the polyene chain to rotate around the C−C bond in order form to a more stable helix or to elongate the chain in order to relieve the steric interactions (Figure 2). Finally, if the substituents on the helical polymer are adequate to induce aggregation spontaneously or under a stimulus, macroscopically chiral aggregates can be obtained.

In summary, PPAs offer a helical (chiral) scaffold with a high degree of control of its sense and elongation that can be easily

functionalized to carry a wide variety of functions and substituents with the ability to induce aggregation into the different types of supramolecular structures described in the following sections according to their morphology.

3. FIBERS, SUPERHELICES, AND DOUBLE HELICES

Helical poly(phenylacetylene)s can self-assemble into fiberlike structures by supramolecular interactions between the pendants of different chains. This aggregation requires the presence of adequate functional groups in the pendant as well as a certain complementarity between the interacting chains. A good example of the role of these two factors is represented by the formation of stereocomplexes through the interaction of stereochemically complementary stereoregular polymers.

In the field of PPAs, there is only one example, reported by Riguera and co-workers, describing a fiberlike stereocomplex. The starting polymers are helical PPAs carrying (*R*)- and (*S*)-α-methoxy-α-trifluoromethyl-α-phenylacetamide pendant groups [poly-(*R*)-**1** and poly-(*S*)-**1**; Figure 3a]. When these polymers are dissolved in tetrahydrofuran (THF), the amide groups are in the cis conformation.[32] In this way, the external crests of the polymer chains are decorated with functions ready for cooperative supramolecular hydrogen bonding with the matching enantiomeric helices (Figure 3b).[54] The interlocking of the chains gives rise to supramolecular fiberlike aggregates that at higher concentrations result in gels (Figure 3c). Modification of the cis−trans conformation of the amide by changing the temperature or solvent polarity allows the controlled formation and cleavage of the stereocomplex due to dramatic changes in the intermolecular and intramolecular hydrogen-bonding interactions.[54]

Apart from that stereocomplex, many other PPAs have been reported to form fiberlike aggregates; in some of these the helicity of the constituting PPA chains is conserved, while in others the aggregation entails the disappearance of the helix. An interesting example of the first class, poly(4-carboxyphenylace-tylene) (poly-**2**), was reported by Yashima and co-workers.[55] This polymer is known to suffer efficient helical amplification to a specific helical sense upon the addition of a small amount of a chiral amine that binds to the carboxyl group. When the
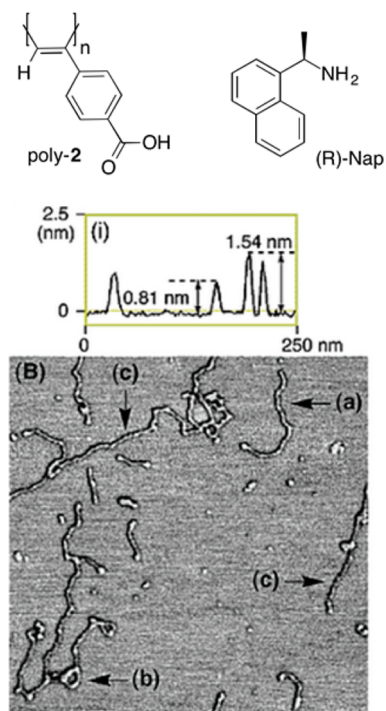
Figure 4. AFM image of poly-**2** complexed with (*R*)-(+)-1-(1-naphthyl)ethylamine [(*R*)-Nap], indicating the presence of single and double helices. Adapted from ref 55. Copyright 2003 American Chemical Society.

amplified PPA was deposited on mica and the resulting monolayer was observed by AFM, some two-helix bundles were found, most probably formed by hydrogen bonding between the carboxyl groups of two different helical chains (Figure 4).[55]
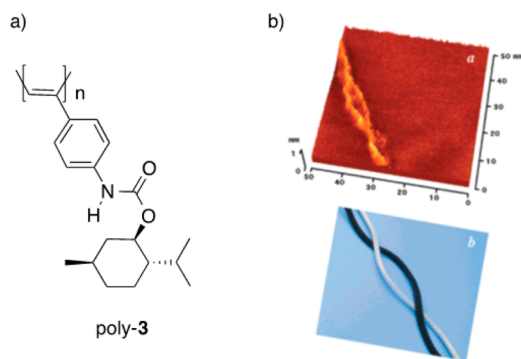

Figure 5. (a) Structure of poly-**3**. (b) Low-current STM height image of two intertwined PPA chains on HOPG at room temperature (top) and a string model of the intertwining polymer chains (bottom). Adapted from ref 56. Copyright 2001 American Chemical Society.

Another example showing the presence of double helices based on PPAs was reported by Shinohara, Shigekawa, and co-workers.[56] They observed by scanning tunneling microscopy (STM) that when a solution of an optically active PPA bearing menthoxycarbonylamino groups (poly-**3**; Figure 5a) was drop-cast onto highly oriented pyrolytic graphite (HOPG), double-helical structures were formed. Although the study showed the presence of single polymer chains, a double-helix structure was predominant on the surface of the substrate (Figure 5b). The researchers also observed that the molecules of the polymer

deposited on HOPG were easy to move by the effect of the probe scanning. In fact, the changes suffered by the macromolecules during the STM measurement made the helical structure become loosened. The authors used this result to point out the need to develop methods to fix the molecules on the substrate in order to get structurally representative STM measurements.
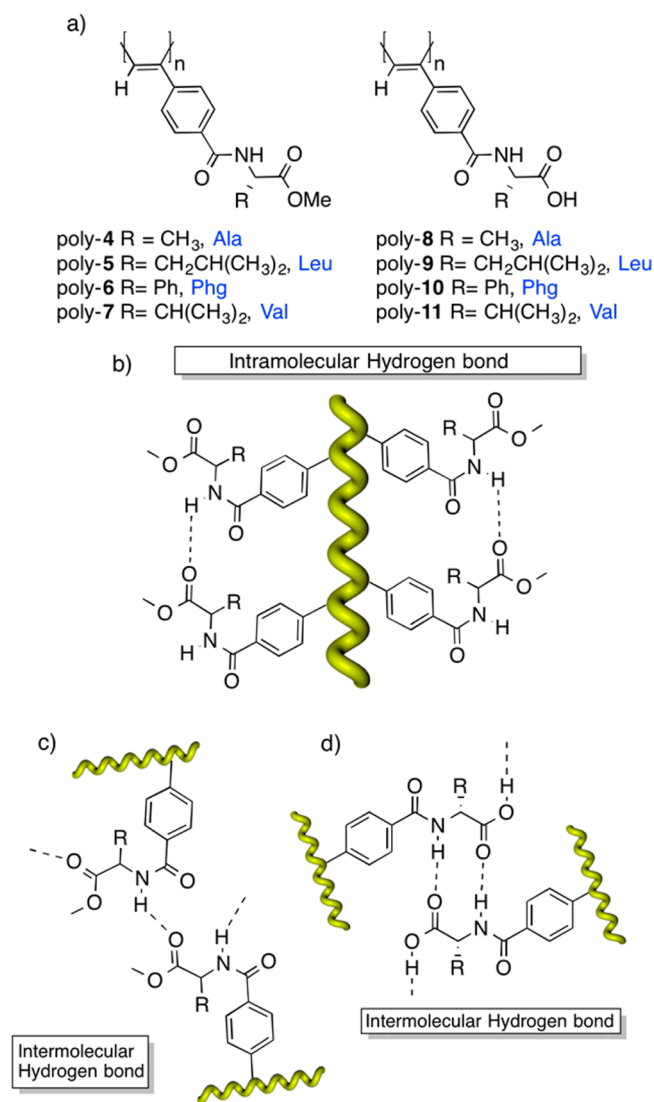
Figure 6. (a) Structures of PPAs bearing amino acids as pendant groups.[31,35,36,57−63] (b) Schematic representation of the intermolecular hydrogen bonds between different pendant groups stabilizing the helical structure of the PPA. (c, d) Schematic representations of the intermolecular hydrogen bonds between the pendant groups of different helices responsible for the formation of high-order aggregates.

Similarly, Tang's group studied the supramolecular interactions originating in helical poly(phenylacetylene)s containing as pendant groups different amino acid residues such as alanine,[35,57] leucine,[58,59] valine,[60−63] or phenylglycine[31] (also studied by Riguera's group[36]) (Figure 6a). In this study, each molecule of the amino acid was attached to the poly(phenylacetylene) backbone through an amide linkage between the amino group of the amino acid and the carboxyl group of the *p*-ethynylbenzoic acid, while the C-terminus of the amino acid was conserved either free (−COOH) or protected as the

methyl ester (−COOMe) (Figure 6a,b). NMR analysis of that series showed that at high concentrations in nonpolar solvents, the pendant groups of all of those polymers tend to form intermolecular hydrogen-bonding interactions. In good agree-

Figure 7. (a, b) AFM images of (a) pearl-like and (b) fiberlike structures obtained upon solvent evaporation of (a) me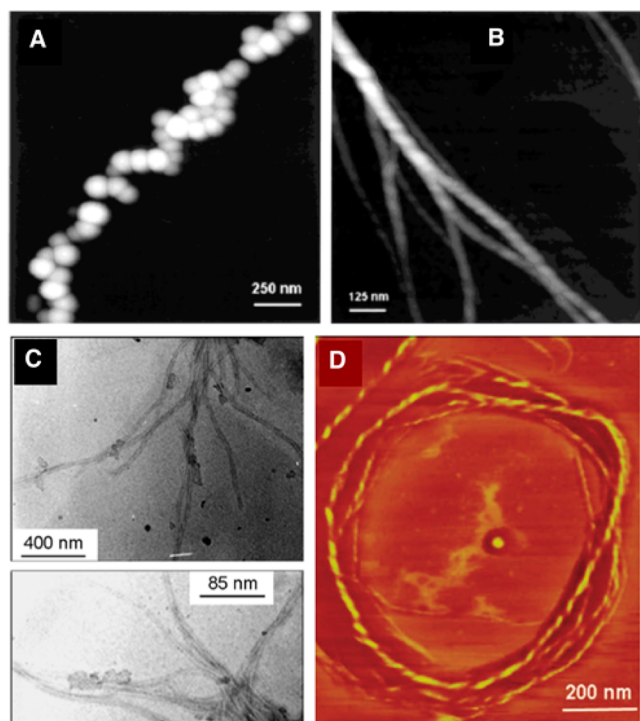thanol and (b) THF solutions of poly-**7**. (c) TEM images of helical nanotubes obtained from natural evaporation of a methanol solution of poly-**4**. (d) AFM image of superhelical ribbons with left-handed twists formed by natural evaporation of a THF solution of poly-**4**. Adapted from (a, b) ref 61, (c) ref 35, and (d) ref 57. Copyright 2003, 2008, and 2012 American Chemical Society, respectively.

ment with that, AFM demonstrated that when solutions of those PPAs in a nonpolar solvent, usually THF, are slowly evaporated on mica, high-order aggregates such as fibers with different lengths and diameters are formed (Figure 7b,d).[35,57,60−63] The information available suggests that in the PPAs with protected pendants (−COOMe), the supramolecular interaction occurs by hydrogen bonding between amide groups of different chains (C=O···H−N), while in the PPAs with free carboxyl groups at the pendant termini, the aggregation results by association between the amide and carboxyl groups of different helical chains (Figure 6c,d).

Interestingly, when these PPAs are dissolved in polar solvents such as methanol, their amphiphilic character (due to the nonpolar backbone and polar pendants) leads to a different type of aggregation, and micellelike structures (see the next section) with the PPA backbone in the core and the amino acid pendants pointing out to the shell are obtained. The high number of amino acid residues that decorate the outside of these micelles leads them to stick together by hydrogen-bonding interactions, forming larger micelles that eventually collapse to generate fiberlike structures (Figure 7a).[31,35,58,60−63] Transmission electron microscopy (TEM) images indicate that these fibers are hollow and can be considered as helical nanotubes (Figure 7c).

Similar results were obtained with other amphiphilic polymers, particularly when groups with well-known self-assembly properties were introduced as pendants. In this way, oligo(phenylacetylene)s containing the nucleoside uridine
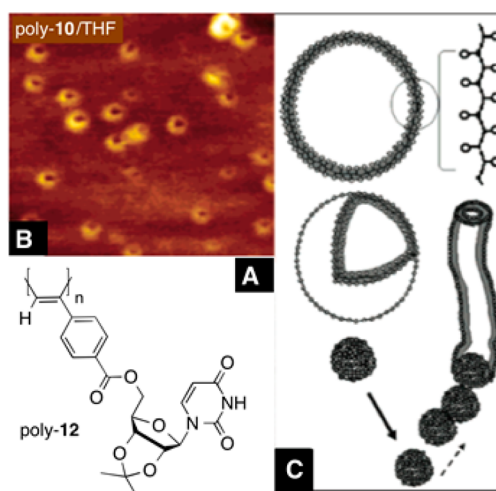

Figure 8. (a) Structure of poly-**12**. (b) Vesicles obtained by natural evaporation of a THF solution of poly-**12**. (c) Schematic representation of the fiberlike aggregates obtained from collapse of the vesicles. Adapted from ref 64. Copyright 2004 American Chemical Society.

(poly-**12**) were synthesized and shown to generate vesicles that stack one on top of the other to form vesicle fibers.[64] This self-assembly originates from the strong hydrogen-bonding interactions promoted by the uridine groups on the different polymeric chains (Figure 8).

Some examples have been reported in the literature where the aggregation of the PPA is not related to its helical structure but occurs only if the polymer adopts a planar structure. Yashima and co-workers have found a very efficient way to force a helical polyenic chain to come close to planarity, consisting of the introduction of repulsions among the pendants either by increasing their size (steric hindrance) or by introducing charges. A representative example of planar-mediated aggregation induced by the size of the pendants is provided by a cyclodextrin-bearing PPA (Figure 9). This polymer adopts an extended almost-planar structure because of the bulkiness of the cyclodextrins, leading to the formation of fiberlike aggregates.[65]

In the second approach, the planarity is induced by the introduction of electric charges on the pendants whose repulsion shifts the original helix to the planar aggregation-prone structure. The easiest way to introduce charges in the polymer consists of the addition of small molecules that interact with the pendants through acid−base or host−guest interactions. In one of those examples, Yashima and co-workers described poly-**18**, a PPA bearing *N,N*-diisopropylaminomethyl groups as pendants (Figure 10a), that aggregated upon the addition of a small amount of a carboxylic acid. This PPA originally had a helical structure, but protonation provoked repulsion between the positively charged pendants that forced the helical backbone to stretch into a planar structure that aggregated into fibers.[66]

In another example reported by the same group, host−guest supramolecular interactions were used to generate supra-molecular helical aggregates. To this end, the PPA poly-**19**
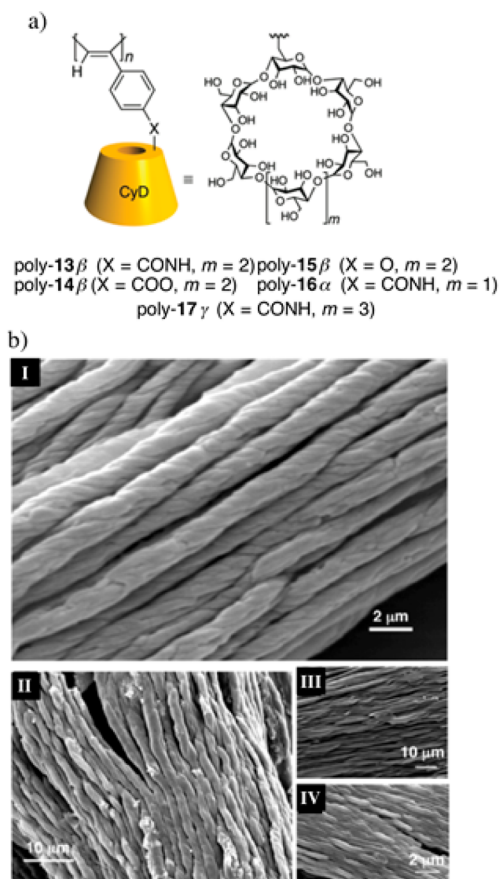
Figure 9. (a) Structures of PPAs bearing cyclodextrin (CyD) pendant groups. (b) SEM images of self-assembled aggregates of (I) poly-**13β**, (II) poly-**15β**, (III) poly-**16α**, and (IV) poly-**17γ**. Reproduced from ref 65. Copyright 2011 American Chemical Society.

Figure 10. Structures of PPAs bearing (a) *N,N*-diisopropylamino-methyl[66] and (b) aza-18-crown-6-ether[67] pendant groups. (c) Schematic representation of (i) chiral amplification in poly-**19** upon complexation with D-Trp followed by addition of the achiral benzoxazole cyanine dye **O-20** and the formation of the corresponding supramolecular helical aggregate of achiral **O-20** with the helical cavity of poly-**19** in acidic water and (ii) memory of the supramolecular chirality after helicity inversion of poly-**19** by excess L-Trp. Panel (c) is reproduced from ref 67. Copyright 2007 American Chemical Society.

incorporating bulky aza-18-crown-6-ether pendants (Figure 10b) was used. Addition of L- or D-amino acids formed host–guest complexes, forcing the polymer to adopt a one-handed helix. As pointed out by the authors, it is important for the aggregation of complexed poly-**19** that its structure presents two well differentiated regions: an external one, over which the aza-18-crown-6-ether complex with the amino acid presides, and one close to the backbone, defined by its hydrophobicity.[67]

In the presence of an achiral benzoxazole cyanine dye, the PPA–amino acid complex acts as a template, with the benzoxazole molecules accommodated on the hydrophobic cavity of the backbone (Figure 10c). The presence of a helical J-aggregate was demonstrated by the existence of induced circular dichroism (ICD) observed in the cyanine dye chromophore region. Interestingly, the helical structure and sense of the J-aggregate showed a memory effect, remaining unchanged even when the helical sense of the PPA–amino acid complex was inverted by addition of the enantiomeric amino acid (Figure 10c).[67]

Other one-dimensional nanostructures that resemble nano-fibers are nanobelts, and PPAs have also been used as starting polymers to produce that type of aggregate. Thus, Wang, Song, and co-workers developed a protocol to generate a PPA-derived nanobelt.[68] It is based on the polymerization of phenylacetylene monomer in the vapor phase catalyzed by cooper nanoparticles (100 nm). In this way, a highly crystalline PPA with the cis configuration of the double bonds is produced and deposited

Figure 11. (a) SEM image of the PPA array. (b) Cross-sectional SEM view of the PPA array. (c) High-resolution SEM image of the PPA nanobelt array. (d) TEM study of an individual PPA nanobelt. Reproduced from ref 68. Copyright 2007 American Chemical Society.

on the inner walls of the flask, forming long ribbons with a typical size of 135 nm (width) × 24 nm (thickness) × 20 mm
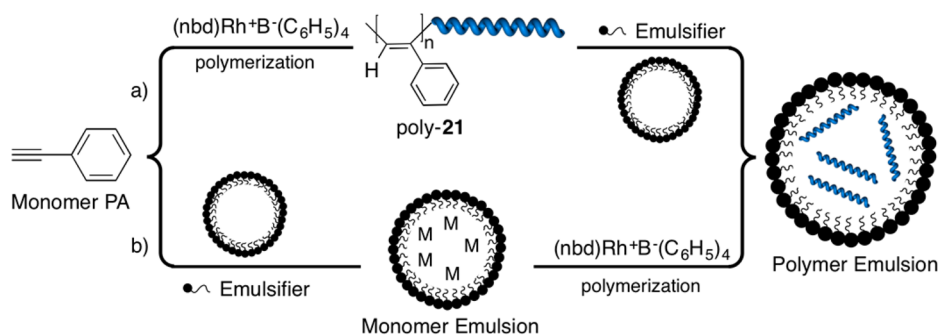
Figure 12. Schematic representation of polymer nanoparticle formation via (a) emulsion of preformed polymers or (b) emulsion polymerization.[70,71]

(length) (Figure 11).[68] These nanobelts have been shown to have semiconductor properties, suggesting potential applications as nanodevices.

4. POLY(PHENYLACETYLENE) NANOCAPSULES, NANOSPHERES, NANOTUBES, AND TOROIDS

The term *polymer nanoparticle* is generally applied to nanospheres or nanocapsules made from any type of polymer and having a size in the range 10−1000 nm. Nanospheres are spherical and solid, and they are frequently used to adsorb molecules on their surface or encapsulate them within the interior. Nanocapsules are colloidal particles consisting of a hollow core surrounded by the polymeric cover. These vesicles are in general employed to encapsulate substances into their cavity.[69]
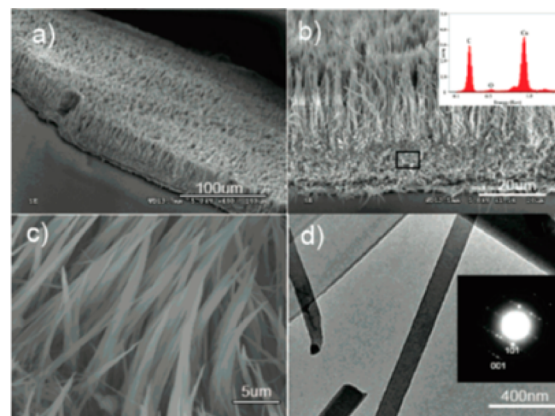
We have already shown in the previous section that helical PPAs containing amino acids or nucleotides as pendants can produce vesicles that collapse to form fiberlike structures.[31,35,58,60−63] In order to obtain nanoparticles from polyacetylenes, two main strategies have been described: one involves formation of the nanoparticles by dispersion of a preformed polymer (the emulsification method), and the other involves polymerization of the monomers under experimental conditions that directly produce the nanoparticles (emulsion polymerization).[70,71] These two approaches are illustrated in Figure 12, and literature examples of their applications to PPAs are given next.

Using emulsification of a preformed helical polymer, Deng and co-workers prepared nanoparticles of poly-(phenylacetylene) (poly-**21**) by dropwise addition of a concentrated THF solution of poly-**21** to a solution of the surfactant sodium dodecyl sulfate (SDS) in deionized water. They found that the diameter of the resulting nanoparticles is highly dependent on the emulsifier concentration: the higher the concentration, the lower is the particle size. They suggested that this is related to the formation of higher number of SDS micelles in the medium.[72]

The same group also explored the emulsion polymerization method. This requires water, a monomer with low water solubility, a water-soluble initiator, and a surfactant. Deng and co-workers applied this method to a series of substituted acetylene monomers and produced nanoparticles with sizes of around 10^2 nm.[73] In most cases, the resulting polyacetylenes have a preference for a helical sense, and therefore, the resulting nanoparticles are chiral.[74]

Macroscopically racemic poly(phenylacetylene) particles were also described by the same group. In that case, the generation of the micelles is related to the presence of an

emulsifier such as SDS or Triton X-100 in water. The liquid nature of the phenylacetylene monomer renders unnecessary the use of an organic solvent to predissolve it, and in fact, it gets dispersed into the micelles as soon as it is added to the water solution. Moreover, the hydrophobic nature of the [(nbd)-Rh$^+$B$^-$(C$_6$H$_5$)$_4$] (nbd = norbornadiene) catalyst results in its rapid dispersion into the micelles in the aqueous mixture, leading after polymerization to the formation of small-diameter (90 nm) particles.[75]

Huber and Mecking[76] described the preparation of nanoparticles of poly-**21** using variations of the emulsion polymerization approach. Thus, mini- and microemulsion polymerizations were employed to prepare PPA particles using a Pd catalyst. In a typical miniemulsion polymerization, the mixture of the monomer, costabilizer (usually a low-molecular-weight compound), surfactant, and catalyst is submitted to ultrasonic treatment in water.[69] On the contrary, in the microemulsion technique, a thermodynamically stable microemulsion of the monomer containing swollen micelles is prepared and then a water-soluble catalyst is added to start the polymerization, which usually requires the presence of high quantities of surfactant.[69] An important difference between mini- and microemulsion polymerization is that they give nanoparticles with different sizes. Thus, Huber and Mecking obtained
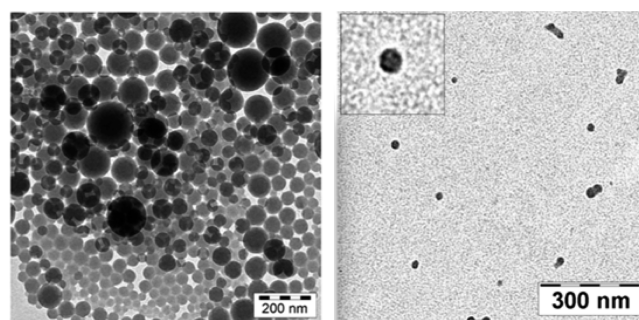
Figure 13. TEM images of poly-**21** particles obtained from (a) mini- and (b) microemulsion polymerization. Adapted from ref 76. Copyright 2010 American Chemical Society.

poly(phenylacetylene) particles with diameters of around 130 nm by miniemulsion polymerization, while microemulsion polymerization of the same polymer gave clearly smaller nanoparticles with diameters of around 25 nm (Figure 13).[76]

Another variation of emulsion polymerization that has attracted the attention of researchers is surfactant-free emulsion polymerization. In the conventional method, the surfactant used during the emulsion polymerization has to be removed

once the particle is obtained. This removal can be a laborious task, and for that reason, surfactant-free alternatives have been developed.[69,77,78] In this field, D'Amato et al.[79] demonstrated that it is possible to obtain poly(phenylacetylene) nanoparticles in the absence of a surfactant if an adequate cosolvent is added. In an example of this approach, the emulsion polymerization of phenylacetylene (PA) in an aqueous medium with the water-

Surfactant free polymerization

Rh(COD)Cl]₂tmeda

toluene/ water

poly-**21**

from 400 to 800 nm
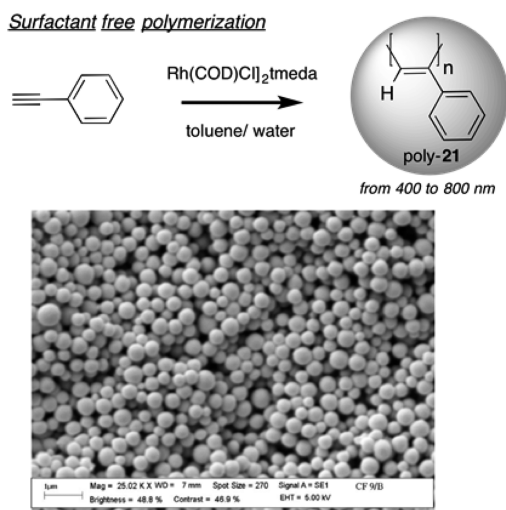
Figure 14. SEM image of PPA particles prepared via surfactant-free polymerization using a PA/toluene mixture. Adapted with permission from ref 79. Copyright 2003 Elsevier.

soluble catalyst $[Rh(cod)Cl]_2(tmeda)$ (cod = *cis,cis*-1,5-cyclo-octadiene, tmeda = *N,N,N′,N′*-tetramethylethylenediamine) was performed in the presence of toluene as the cosolvent (Figure 14). Here toluene plays a dual role: it allows the emulsion to form and permits the size of the droplets to be controlled. Bigger particles are obtained in the absence of toluene, whereas increasing the amount of toluene decreases the monomer droplets and their coalescence probability, therefore resulting in small-dimension and low-polydispersity particles. The results can be explained by assuming that toluene forms a layer around the monomer droplets that stabilizes them and helps to control their size. By means of this technique, beads with diameters of 400−800 nm have been obtained that can potentially be used as photonic crystals.[80]

Following the emulsion polymerization technique developed by D'Amato et al., Russo and co-workers explored different ways to optimize the control over the size and dispersion of the resulting PPA particles. Thus, in a first study they found that when the organometallic catalyst was replaced by a radical initiator such as potassium persulfate (KPS),[81] the polydispersity of the polymer particles decreased as a result of the presence of charged species in the reaction mixture that stabilized the emulsion. Moreover, the size of the particles could also be modulated by modification of the initiator concentration, as the presence of increasing amounts of initiator generated larger particles, although the polydispersity increased because of the higher density of nucleation sites.

In a second approach, Russo and co-workers changed the polymeric system from homo-PPA to a copolymer formed from PA and a charged monomer, 2-hydroxyethyl methacrylate (HEMA).[82] The idea behind this change was that the charged monomer would occupy the outer part of the nanobead, enhancing the stability of the colloids in the water suspension.

The emulsion polymerization of this system also showed possibilities to improve the particle control. In fact, increasing the amount of the initiator led to a decrease in the size of the particles, which was the opposite of the homopolymer approach described before. This apparently surprising result can nevertheless be explained by the slower polymerization of the copolymer, which causes the particle growth to be limited by the size of the polymer chain.

Several studies on the optimization of the size and dispersity of the polymer particles were carried out by Russo and co-workers by modification of the reaction parameters (reaction time, monomer/comonomer ratio, cosolvent, and initiator concentration). Thus, copolymers of phenylacetylene with different hydrophilic comonomers such as acrylic acid or *N,N*-dimethylpropargylamide (DMPA) were prepared, and the different parameters affecting their size and polydispersity were studied.[83,84] In this way, particles with diameters of 50−800 nm and low polydispersities (1.11−1.30) and surface charge densities (0.44−2.87 mC cm^{-2}) were prepared, and their surface compositions were evaluated by semiquantitative X-ray photoelectron spectroscopy analysis.[83,84]

Nanoparticles made from poly(phenylacetylene)s can also be obtained using non-covalent cross-linking agents. Thus, Riguera and co-workers[85−87] converted a PPA bearing either (*R*)- or (*S*)-α-methoxy-α-phenylacetic acid (MPA), connected to the phenylacetylene through a C_6H_4−NH−C(═O) amide bond, into nanospheres by addition of a solution of mono- or divalent metal ions (added as perchlorate salts in THF). The polymers [poly-(*R*)- and poly-(*S*)-**22**] dissolved in different organic solvents [$CHCl_3$, CH_2Cl_2, *N,N*-dimethylformamide (DMF), acetone, THF, dimethyl sulfoxide (DMSO)] are composed of equal amounts of left-handed (*M*) and right-handed (*P*) helices in rapid equilibrium showing null CD (Figure 15b). Nevertheless, their left- or right-handed helical sense can be amplified selectively by addition of mono- or divalent metal ions, respectively [e.g., the left-handed helical sense of poly-(*S*)-**22** is amplified when a perchlorate salt of a monovalent metal is added, while the right-handed helical sense is amplified when the perchlorate salt of a divalent metal ion is added; Figure 15a]. The metal ion can act not only as helical inducer but also as a cross-linking agent, generating nanospheres whose size and chiral content can be controlled by the polymer/metal ratio and the solvents used to dissolve the polymer and the metal ion (Figure 15b,c). The encapsulation ability of these nanospheres was demonstrated by encapsulation of iron oxide magnetic nanoparticles, quantum dots, or organic molecules such as fluorescent dyes (Figure 15d).[86,88,89]

Moreover, by variation of the solvent, these poly-**22**/monovalent metal ion complexes can be converted into other types of nanostructures: nanotubes are formed when a cosolvent with a high boiling point is added, while toroidal nanostructures are obtained upon addition of a solvent in which the polymer is poorly dissolved (Figure 16).[88]

Finally, using the formation of nanospheres by complexation with monovalent and divalent metal ions as a test, the same group evaluated the "sergeants and soldiers" effect in a number of copolymers formed by a monomer containing MPA as the chiral constituent (the "sergeant") and a variety of achiral monomers (the "soldiers"). They found that when the achiral component of the copolymer was the 4-ethynyl anilide of either phenylacetic acid or diphenylacetic acid, the "sergeants and soldiers" effect can be activated/deactivated by the presence/absence of the metal ion, allowing the generation of
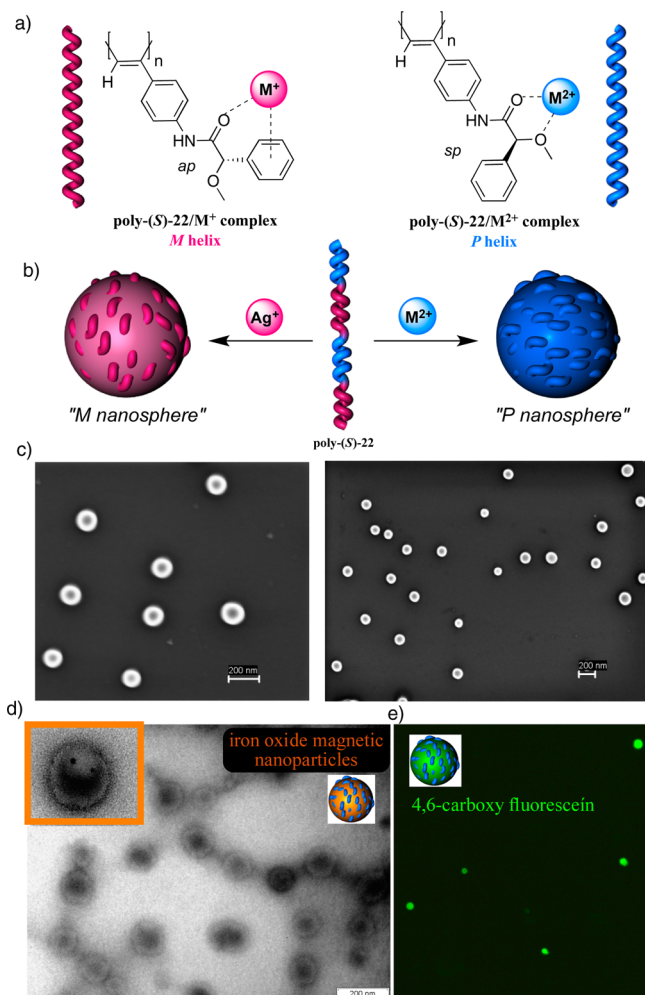
Figure 15. (a) M and P helices induced in poly-(S)-22 by the addition of mono- and divalent metal ions, respectively. (b) Schematic representation of the chiral nanospheres obtained by complexation of poly-(S)-22 with mono- or divalent metal ions. (c) Field-effect SEM images of helical polymer−metal complex (HPMC) nanospheres (scale bars = 200 nm). (d) TEM images of HPMC nanospheres encapsulating iron oxide nanoparticles (scale bar = 200 nm). (e) Confocal microscopy image of HPMC nanospheres encapsulating 5,6-carboxyfluorescein (λ_{exc} = 495 nm, λ_{em} = 505−540 nm). Adapted from ref 89. Copyright 2012 American Chemical Society.

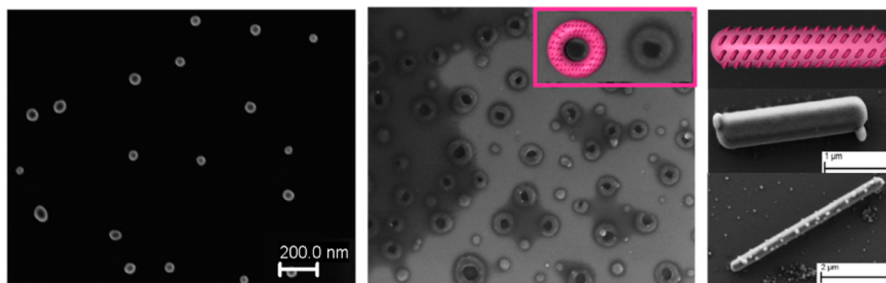nanospheres formed by left- or right-handed polymeric helices depending on the valence of the ion added (Figure 17).[90]

5. CHIRAL STIMULI-RESPONSIVE POLY(PHENYLACETYLENE) GELS

A stimuli-responsive gel was developed by Yashima and co-workers[91] by covalent cross-linking of a PPA formed from (4-carboxyphenyl)acetylene as the monomer. The cross-linking was carried out following two different strategies: (1) using a bis(phenylacetylene) derivative as the cross-linking agent (gel-24) and (2) cross-linking the poly(4-carboxyphenyl)acetylene with a diamine (gel-25) (Figure 18). Conversion of the carboxy groups into sodium carboxylates allowed the gels to swell in DMSO or water. The gels were shown to respond to the presence of chiral amines that interact with the carboxyl groups of the PPA, forcing the chain to adopt a specific helical sense.

6. LAYER-BY-LAYER ASSEMBLY OF POLY(PHENYLACETYLENE)S

Layer-by-layer (LBL) assembly of charged polymers is a very useful technique to generate multilayer films by interactions between polyanions and polycations. The functionality of poly(phenylacetylene)s, their helicity, and the possibility to control their helical sense by external stimuli make PPAs very attractive starting materials to produce chiral LBL functional films.

In a very interesting paper, Yashima and co-workers prepared three different LBLs based on mixtures of (a) an anionic PPA (bearing phosphonate groups as pendants) with a poly-(allylamine), (b) a cationic PPA (with ammonium groups as pendants) with poly(acrylic acid), and (c) the anionic phosphonate-bearing PPA with the cationic ammonium-bearing PPA (Figure 19).[92] All of those polymers are achiral but can be induced to adopt a specific helical sense by addition of a chiral external stimulus (a chiral amine or a chiral carboxylic acid) that binds to the PPA. When the corresponding counterion polyelectrolyte [poly(allylamine) or poly(acrylic acid)] is added to these helical-induced anionic or cationic PPAs, the polyelectrolyte replaces the chiral stimulus agent, generating an LBL assembly with macromolecular helicity memory, meaning that the chirality induced in the PPA by the external stimulus is retained in the resulting LBL assembly (Figure 19).[92]

7. TWO-DIMENSIONAL CRYSTALS

When organic molecules are deposited on solid substrates (mica, graphite, Si wafer), the weak intramolecular, intermolecular, and/or interfacial interactions become important enough to cause the formation of supramolecular structures by self-assembly of individual small molecules, macromolecules, or polymers. This process is important in the development of
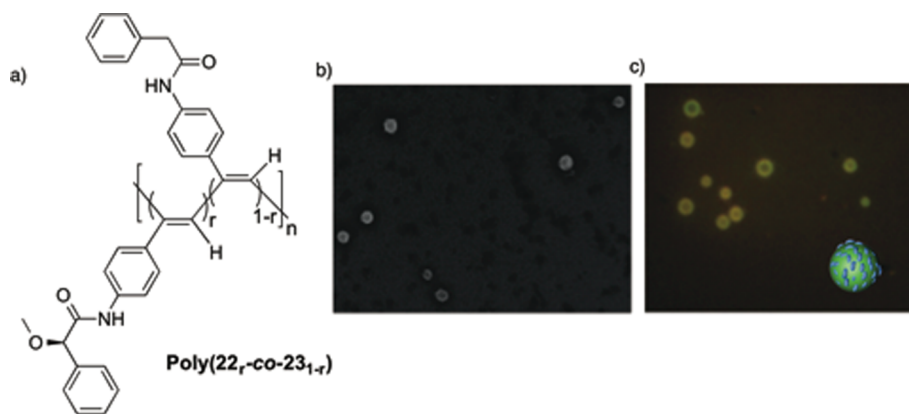

Figure 16. SEM images of different nanostructures (nanospheres, toroids, and nanotubes) obtained from HPMCs. Adapted with permission from ref 88. Copyright 2014 Wiley-VCH.

Figure 17. (a) Designed PPA copolymer that follows the "sergeants and soldiers" effect when a monovalent or divalent metal ion is added. (b) SEM and (c) confocal microscopy images of the copolymer–Ba^{2+} metal complex. Adapted with permission from ref 90. Copyright 2014 Royal Society of Chemistry.
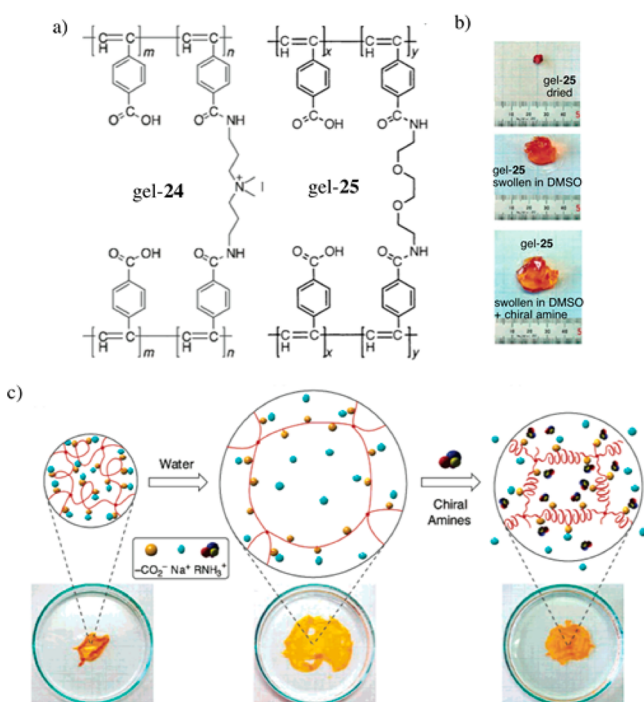

Figure 18. (a) Structures of gel-**24** and gel-**25**. (b) Photographs of gel-**24** in a dried state and in a swollen state in DMSO in the absence or presence of a chiral amine. (c) Schematic illustration of swelling and shrinking of gel-**25**-Na derived from gel-**25** in water after the addition of chiral amines (top) and changes in the volume of gel-**25**-Na with a chiral amine in water (bottom). Adapted from ref 91. Copyright 2003 American Chemical Society.

Figure 19. Schematic illustration of the LbL self-assembly of charged poly(phenylacetylene)s with induced macromolecular helicity. (a) An excess of the one-handed helical sense is induced in poly-**26** and poly-**27**-HCl upon complexation with optically active (S)-**28** and (S)-**29**, respectively. (b) Helical-induced poly-**26** and poly-**27**-HCl can be LbL-assembled with achiral polyelectrolytes with opposite charges (PAA and PAH), resulting in multilayer thin films with an induced macromolecular helicity on a substrate. Reproduced from ref 92. Copyright 2005 American Chemical Society.

hot fields such as functional coatings, biomaterials, electronics, and sensors, among others. In general, the morphology of these supramolecular structures is available using techniques of surface analysis such as STM, scanning probe microscopy (SPM), and AFM, which under optimal conditions can be used to obtain high-resolution images of single molecules, their conformations, and organization in the layers.

Apart from the nanoparticles, fibers, gels, toroids, and belts mentioned in the previous sections, PPAs have also been shown to generate 2D crystals when deposited on certain solid supports. This topic has attracted the attention of some research groups, and we will show in this section the most relevant results, paying particular attention to the helicity of the

PPAs and its transfer to the supramolecular arrangement. This is particularly important in this class of supramolecular structures because the interactions with the solid surface of the support can compete so strongly with the intermolecular assembly that the original helical conformation results are modified when the 2D crystal is formed.[93] This fact stresses the importance of the selection of the support and the method of 2D layer formation.

Yashima and co-workers[94] undertook the study of PPAs bearing bulky groups by AFM. More precisely, they analyzed cis–transoidal copolymers containing an achiral C$_{60}$-bound phenylacetylene and an optically active pendant, i.e., an (R)-[(1-phenylethyl)carbamoyl]oxy substituent (Figure 20a). This copolymer, poly(**30**$_m$-co-**31**$_n$), was deposited on freshly cleaved mica and on HOPG, and the morphologies of the assemblies were studied by AFM. The AFM images on mica (cast from
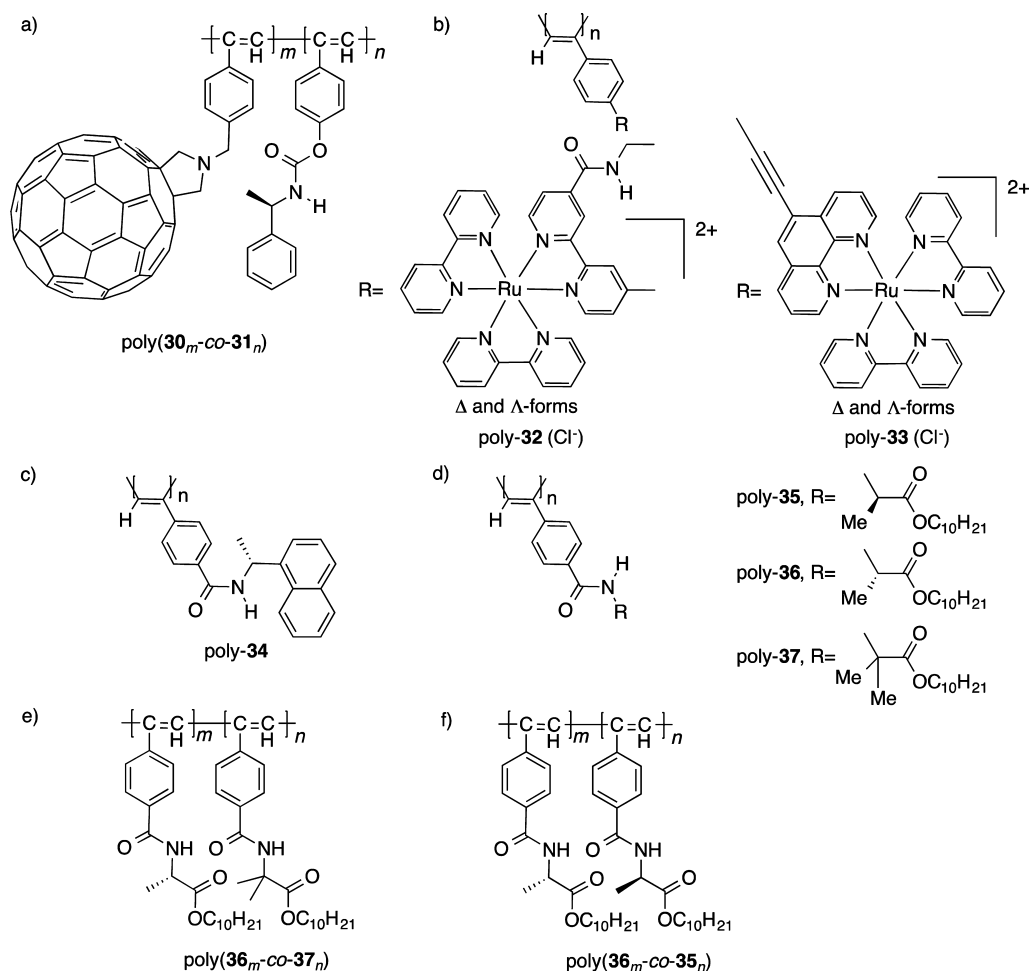
Figure 20. Structures of (a) poly(30$_m$-*co*-31$_n$);[94] (b) poly-**32** and poly-**33**;[95] (c) poly-**34**;[55] (d) poly-**35**,[34,93] poly-**36**,[34,93] and poly-**37**;[97] (e) poly(36$_m$-*co*-37$_n$);[98] and (f) poly(36$_m$-*co*-35$_n$).[99,100]

THF) showed isolated particles originating from aggregation of the C$_{60}$ groups in clusters as a result of the repulsion between the hydrophobic C$_{60}$ units and the hydrophilic mica substrate. Nevertheless, deposition of the copolymer on HOPG instead of mica led to images showing extended and individual copolymer chains together with some isolated particles. These results indicate that the attractive force between the pendant fullerene groups and the solid substrate plays a critical role in the morphology of the C$_{60}$-based polymers and suggest that the interplay between the hydrophobic/hydrophilic nature of the support and the pendants of the polymer can be used to select a certain class of suprastructure.

In a related example, helical PPAs poly-**32** and poly-**33**, each bearing the two chiral forms of a bulky ruthenium complex as pendants, were prepared (Figure 20b), and the supramolecular structures formed by deposition on mica were investigated by AFM.[95] The polymers adsorbed on mica clearly showed isolated strands, and visualization of the right- and left-handed helices of the polymers was possible by high-resolution AFM. Nevertheless, when low- and high-molecular-weight poly(4-carboxyphenylacetylene)s (poly-**2**) and their complexes with (*R*)-(+)-1-(1-naphthyl)ethylamine [(*R*)-Nap] (Figure 4) and an optically active PPA with that amine covalently bonded as the pendant (poly-**34**; Figure 20c) were deposited on mica,[55] AFM showed single chains of the polymer, but the helical sense could not be determined.

In another series of papers,[34,93,96−99] the Yashima group reported on the self-assembly behavior of helical PPAs bearing L- or D-alanine residues with long alkyl chain (i.e., C$_{10}$H$_{21}$) pendants (Figure 20d). In a first communication,[93] they reported that these cholesteric liquid-crystalline helical PPAs[100] deposited on HOPG self-assembled into ordered 2D layered crystals. Flat monolayers epitaxially formed on the basal plane of the graphite were observed (Figure 21a). The rodlike helical chains were visualized by AFM, while X-ray diffraction (XRD) analysis of the oriented liquid-crystalline polymer films allowed quantification of the molecular packing, helical pitch, and handedness.

A remarkable result was the preparation of switchable 2D chiral surfaces.[34] This was achieved by inversion of the helicity of the 2D-crystal-forming PPAs by exposure to specific organic solvents (Figure 21b), which also allowed control of the helical sense in mesoscopic cholesteric states.[96] The resulting 2D self-assembled polymer bundles (spin-cast on HOPG from THF) were visualized by AFM with molecular resolution (Figure 21c).[34]

Subsequent reports further explored the 2D aggregation of related polymers. The dynamically racemic PPA poly-**37** bearing achiral pendants, i.e., α-aminoisobutyric acid (Aib) *n*-decyl esters (Figure 20d), also crystallized under an organic solvent atmosphere on HOPG, resulting in 2D helix bundle formation.[97] Enantiomeric right- and left-handed helical
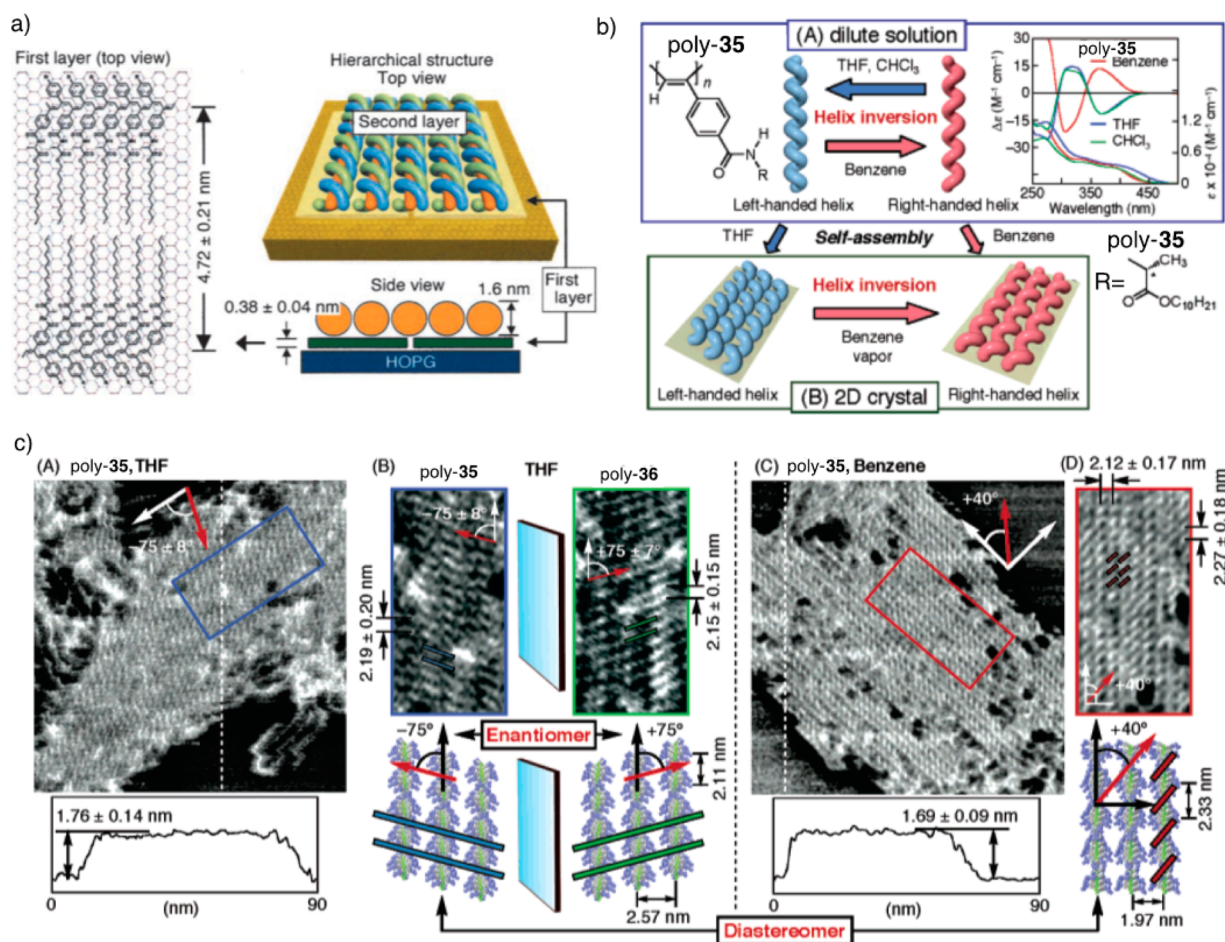
Figure 21. (a) Schematic representation of the hierarchical structure of the self-assembled poly-**36** on HOPG. Adapted with permission from ref 93. Copyright 2006 Wiley-VCH. (b) Schematic illustration of the macromolecular helicity inversion of poly-**35** in dilute solution and the 2D crystal state. (c) AFM images of 2D self-assembled poly-**35** and poly-**36** on HOPG and their helical structures proposed by AFM and XRD analyses. Adapted from ref 34. Copyright 2006 American Chemical Society.

segments and helical reversals were visualized by high-resolution AFM on HOPG, and the results were quantified by XRD analysis of an oriented poly-**37** liquid-crystalline film.

New PPAs with different combinations of *n*-decyl pendants were also prepared, and their 2D assemblies were studied. High-resolution AFM images of optically active copolymers bearing L-alanine decyl esters and Aib decyl esters as pendants (Figure 20e)[98] on HOPG showed the formation of self-assembled 2D helix bundles (Figure 22a). Almost no chiral amplification of the macromolecular helicity was observed for homopolymer mixtures, i.e., poly-L-alanine decyl ester (poly-**36**) and poly-Aib (poly-**37**), in either the liquid-crystalline state or 2D crystals on graphite, but it was increasingly amplified in the copolymers when going from the solution state to the liquid-crystalline state and to the 2D crystal state (Figure 22b).

Analogous studies[99] were carried out with PPA copolymers bearing L- and D-alanine decyl esters as the side groups [poly(36_m-*co*-35_n); Figure 20f]. In this case, amplification of the helical-sense excess (i.e., the majority rule effect) was shown by AFM to operate to similar degrees in both the cholesteric liquid-crystalline state and in 2D crystals deposited on graphite.

Other research groups also studied the 2D aggregation of PPAs bearing amino acid pendants. Tang and co-workers[57,60] examined the self-assembly of PPAs carrying L-valine (poly-**7**) and L-alanine (poly-**4**) methyl esters (Figure 6a) in monolayers

prepared by the Langmuir–Blodgett film technique on a water surface and later deposited on mica and visualized by AFM. Poly-**7**[60] chains were shown to assemble into a monolayer of extended fibers, but no helical information could be obtained from these 2D aggregates. As a consequence of the results with poly-**7**, the same group studied the ability of poly-**4** to form self-assembled structures at the air–water interface.[57] In this case, they found that the majority of the surface was covered with a layer of flat film with well-ordered parallel ridges, indicating that the polymer maintains its helical conformation within the monolayer (Figure 23).

As part of their extensive studies on helical polymers, Percec et al.[101] prepared cylindrical cis–transoidal poly(arylacetylenes), i.e., poly(2-ethynyl-9-substituted carbazole)s (poly-**38** and poly-**39**) and poly(3-ethynyl-9-substituted carbazole)s (poly-**40** and poly-**41**), containing chiral and achiral minidendritic substituents (Figure 24a). Among other structural studies on these macromolecules, they were able to visualize individual chains of one of those polymers by AFM. In those experiments, they carried out spin-casting on graphite accompanied by thermal annealing at 100 °C (Figure 24 b–e).

This group also prepared a library of 11 PPAs (poly-**42** to poly-**52**) with a cis–transoidal skeleton and self-assembling dendrons as pendants (Figure 25).[102,103] They observed that the polymer backbone serves as a helical scaffold for the
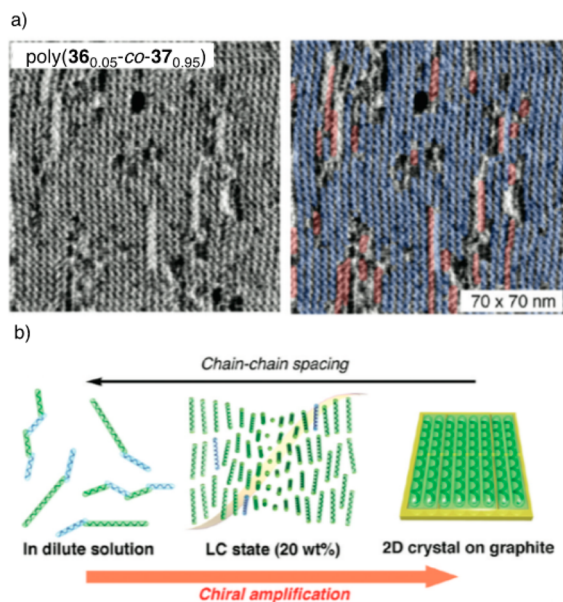
Figure 22. (a) AFM phase images of 2D self-assembled poly($36_{0.05}$-*co*-$37_{0.95}$) cast from dilute toluene solutions on HOPG. (b) Schematic illustration of hierarchical chiral amplification of macromolecular helicity of poly(36_m-*co*-37_n). An excess of one-handed helical sense (right- or left-handed helix) is significantly amplified in the liquid-crystalline state and further amplified in the 2D crystal, resulting from cholesteric liquid crystal and 2D helix bundle formation, respectively. Adapted from ref 98. Copyright 2011 American Chemical Society.
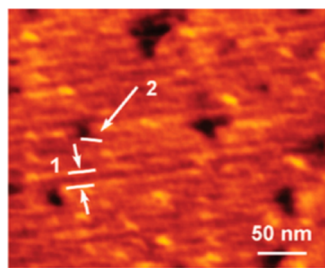

Figure 23. High-resolution image of the aligned polymer chains at the air−water interface. Adapted from ref 57. Copyright 2012 American Chemical Society.

amphiphilic self-assembling dendrons and that the dendron primary structure dictates the diameter of the cylindrical PPAs. This role of the primary dendron is operative in the bulk, in both the self-organized hexagonal columnar lattice (as determined by XRD) and the monolayers deposited on HOPG and mica (as visualized by AFM) (Figure 26).

A detailed AFM study of one of those dendronized PPAs (i.e., poly-**47**) deposited on HOPG (Figures 26 and 27a)[103] showed individual macromolecules as oblate cylindrical objects. Their orientation in the first layer, directly adsorbed on the HOPG, reflected the underlying lattice symmetry as a result of the adsorption of the long alkyl tails. Another consequence of epitaxy was that at the HOPG interface, the PPA backbone adopted a more extended conformation than in the hexagonal columnar phase found in the bulk. Finally, it was found that thermal annealing induced intermolecular interactions that resulted in large domains of oriented dendronized chains (i.e., 2D nematic order) (Figure 27b,c).

In our studies on the control of the helicity and aggregation of PPAs by complexation with mono- and divalent metal ions,

several polymers and copolymers bearing short chiral pendants, i.e., phenylglycine methyl ester (poly-**6**; Figures 6 and 28),[36] α-methoxy-α-phenylacetic acid (poly-**22**; Figures 15 and 29),[87] α-methoxy-α-trifluoromethyl-α-phenylacetic acid (poly-**1**; Figures 3 and 30),[32] and poly(**22**$_{0.6}$-*co*-**23**$_{0.4}$) (Figures 17 and 31),[90] were visualized by AFM after they were spin-cast on HOPG. Those studies gave invaluable information on the structure (e.g., width, helical pitch, length) and 2D arrangements of the polymer chains on the graphite surface (Figures 28−31).

8. LIQUID CRYSTALS, ORIENTED FILMS, AND COLUMNAR ASSEMBLIES

Liquid crystals (LCs) formed by polymers (i.e., polymer liquid crystals) are materials that incorporate the properties and characteristics of both liquid crystals and polymeric compounds. As a result, these hybrid materials may present the typical mesophases of LCs together with many of the advantageous properties inherent in their polymeric nature.

In general, polymers with flexible chains and the mesogens (i.e., disklike or rodlike structural moieties) placed either in the polymer backbone or as side chains (i.e., pendants) have been considered more attractive than rigid backbones for the preparation of polymeric liquid crystals.[104] Among the different polymers used to form LCs, polyacetylenes and PPAs with pendants containing mesogenic groups (e.g., biphenyl, phenylbenzoate),[105−108] have been described that demonstrate their potential as LCs, combining liquid-crystallinity with the properties associated with their helicity.

In the past decade, the Tang group faced the challenge of synthetizing side-chain liquid-crystalline polyacetylenes following a rational design based on the introduction of pendants where variations on flexible spacers, functional bridges, mesogenic cores, and flexible or functional tails are combined.[105,106,109−113] In these studies, the structure of the mesogenic pendants was shown to be crucial to get a liquid-crystalline state. For instance, a group of PPAs of general structure poly-**53** (Figure 32) did not exhibit LC properties,[109,110] probably because of the rigidity of the poly(phenylacetylene) backbone and the strong electronic interactions of the polarized [(cyano)biphenylyl]oxy pendants. However, replacing the highly polar cyano group with a less polar alkoxy group (poly-**54**; Figure 32) allowed a smectic A mesophase to be formed.[111]

The critical role played by the different spacers introduced in the pendants was also observed by Hsu.[114] Thus, poly-**55**, which do not contain a flexible spacer (Figure 32), showed no mesomorphic properties, whereas poly-**56** containing three or four methylene units in their spacers (Figure 32) did exhibit both smectic A and smectic C phases.

Other structural variations were explored by Tang, who incorporated cholesteryl (poly-**57**), ergosteryl (poly-**58**), and stigmasteryl (poly-**59**) mesogens in monosubstituted PPAs (Figure 32).[115] All of those polymers showed liquid-crystalline properties: poly-**58** showed nematicity, whereas poly-**57** and poly-**59** formed enantiotropic smectic A mesophases.

More recently, four PPAs bearing the well-known mesogenic azobenzene system were synthesized (Figure 32).[116] The azobenzene and trifluoromethyl-capped azobenzene moieties were linked to the PPA skeleton with flexible alkyl spacers, and their liquid-crystallinity was examined by polarized optical microscopy (POM) (Figure 33). These studies indicated that poly-**60**(12) and poly-**61**(12), both possessing the long −(CH$_2$)$_{12}$− linker, exhibited LC properties, but when that
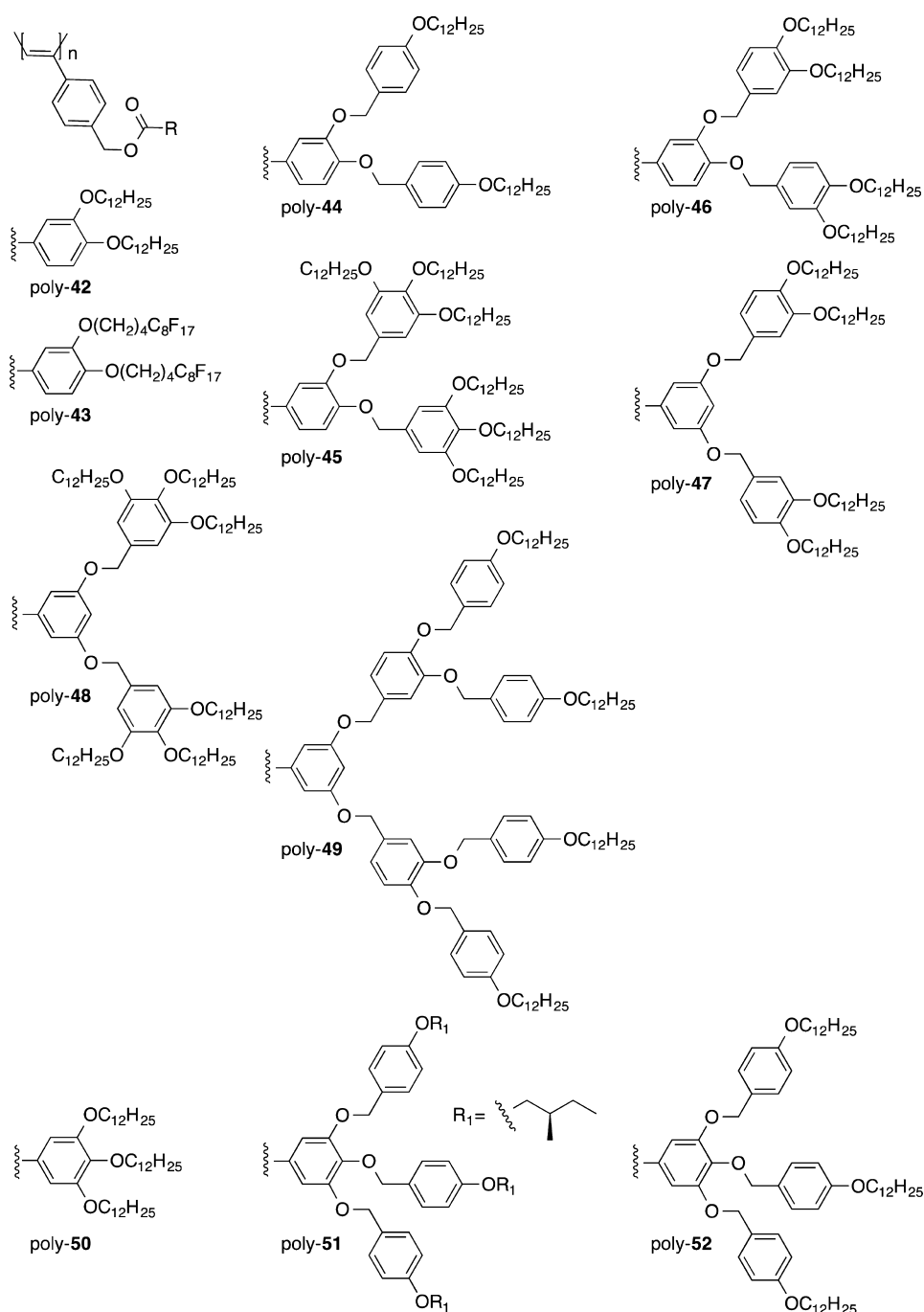
Figure 24. (a) Structures of poly-**38**, poly-**39**, poly-**40**, and poly-**41**. (b) AFM image of the top layer of poly-**40** on graphite after annealing at 100 °C. (c) Height image of the dark region in (b). (d, e) Images of the same region shown in (c) with an elevated tip−sample force. Adapted with permission from ref 101. Copyright 2002 Wiley Periodicals, Inc.

linker was replaced by a shorter one, −(CH$_2$)$_6$−, the resulting polymers poly-**60**(6) and poly-**61**(6) did not present LC properties despite containing the azobezene group. Therefore, it is obvious that the lengh and flexibility of the alkyl spacer plays a key role in the formation of the mesophase. The mesomorphic texture in the POM images suggests that the mesophases formed by poly-**60**(12) and poly-**61**(12) could be assigned as smectic A phases. The molecular arrangement shown in Figure 33d was tentatively proposed for the smectic A structure of poly-**61**(12) on the basis of XRD analysis and theoretical calculations.

Also, a large number of liquid-crystalline disubstituted PPAs incorporating a variety of substituted phenyl groups and long mesogenic pendants have been prepared. Many of those polymers present advanced electrical, light-emitting, and optical properties. Those results, mainly coming from the groups of Tang and Akagi, have already been exhaustively reviewed.[31,115,117−119]

Liquid crystals have also been obtained from PPAs substituted with dendrimers. For instance, Percec's cylindrical cis−transoidal poly(arylacetylenes) containing minidendritic substituents, which were described in the previous section (poly-**38**, poly-**39**, poly-**40**, and poly-**41**; see Figure 24), were shown to exhibit chiral and achiral nematic phases. These phases were studied by thermal optical polarized microscopy (TOPM) and XRD experiments.[101]

Two polymers prepared by Meijer and co-workers,[120] one of them chiral (Figure 34), were also among the first examples of PPAs that behave as liquid crystals. This property is presumably caused by a bilayer-type architecture in which the mesogens incorporating three long alkyl chains, i.e., 3,4,5-tridodecyloxyphenyl and 3,4,5-tris[(S)-3,7-dimethyloctyloxy]phenyl pendants (poly-**62** and poly-**63**, respectively), are disposed in an antiparallel overlapping interdigitated manner.

In studies with water-soluble PPAs, Yashima found that an optically inactive, positively charged polyacetylene, namely, the hydrochloride of poly[4-(N,N-diisopropylaminomethyl)-phenylacetylene] (poly-**27**-HCl; Figures 19 and 35a), showed helical amplification induced by a small amount of a chiral acid, i.e., the sodium salt of (S)- or (R)-phenyllactic acid (**29**), as a dopant in water. In that study, the macromolecular helicity was significantly amplified in the cholesteric liquid-crystalline state

(Figure 35a).[121] On the other hand, it was observed that this PPA formed a lyotropic nematic liquid-crystalline phase in water in the absence of chiral acids and that the neutral polymer showed no liquid-crystalline phase in organic solvents.[122] XRD analysis of the oriented films of the nematic and cholesteric LCs from this PPA showed them to exhibit almost identical diffraction patterns, suggesting that the polymer may have the same helical structure in both cases despite the substantial difference in their helical characteristics (i.e., dynamically racemic and one-handed helices, respectively, in dilute solution). On the basis of those analyses, a mechanism was proposed to explain the chiral amplification and the formation of the liquid-crystalline states (Figure 35b).[122]

A related PPA bearing phosphonic acid monoethyl ester pendants (poly-**26**; Figure 19) showed a similar behavior. In concentrated water solutions and in the presence of optically active amines, this polymer in the acid form and as the sodium salt formed cholesteric and lyotropic nematic liquid-crystalline phases, respectively.[123]

The formation of LCs in organic solvents was also achieved with PPAs. Thus, chiral cis−transoidal PPAs bearing L-, D-, or racemic DL-alanine residues with a long alkyl chain as pendants [poly-**36**, poly-**35**, and poly(**36**$_{0.5}$-co-**35**$_{0.5}$); Figure 20d,f], formed well-defined lyotropic cholesteric or nematic liquid-crystalline phases. The exact phase obtained in each case was shown to depend on the chiral constituent in the pendant, as evidenced by their fingerprint and Schlieren textures (Figure 36).[100] Clear microscopic textures were observed in nonpolar solvents such as 1,2-dichloroethane, benzene, chloroform, 1,1,2,2-tetrachloroethane, and carbon tetrachloride. When those polymers were deposited on solid supports such as graphite, they formed 2D chiral surfaces observable by AFM (see the previous section).[93,96]

A structurally related racemic PPA bearing achiral Aib with the same n-decyl chain as pendants (poly-**37**; Figure 20d) formed a lyotropic nematic liquid-crystalline phase in concentrated benzene solution.[97] Copolymers made by combination of these n-decyl-containing pendants also showed the formation of lyotropic liquid-crystalline states. This behavior allowed the study in dilute solutions, LCs, and two-dimensional crystals (see the previous section) of the hierarchical amplification of macromolecular helicity in PPA

Figure 25. Library of dendronized poly(phenylacetylene)s poly-**42** to poly-**52**.[102,103]

copolymers composed of chiral and achiral pendants[98] [poly(**36**$_m$-co-**37**$_n$); Figure 20e] as well as with nonracemic pendants[100] [poly(**36**$_m$-co-**35**$_n$); Figure 20f].

Liquid-crystalline behavior was found in other PPAs with the same structural characteristics (e.g., the presence of long aliphatic chains). Thus, during the study of the effect of alkyl pendants on the chiroptical properties of optically active PPA films, POM observations revealed that poly-**64** (Figure 37) in CHCl$_3$ solution formed a cholesteric phase. Also, oriented films were obtained from certain solvents and observed by wide-angle XRD (WAXRD). A long hydrophobic chain was necessary to get these aligned structures.[124]

Although the orientational organization of the polymers that leads to the formation of a liquid crystal is usually provoked by the use of concentrated solutions (see previous sections), Yashima and co-workers reported that the uniaxial orientation of a rodlike helical PPA can also be produced by an electric field.[125] In this example, a helical polymer with pendants bearing L-alanine residues with long alkyl chains (poly-**36**; Figure 20d) formed a highly aligned cast film when submitted to an electric field (Figure 38). The oriented film was prepared by gradual solvent evaporation, in a benzene vapor atmosphere, of a concentrated LC benzene solution of the PPA deposited on a CaF$_2$ substrate within an electric field (i.e., 6000 V/cm). The structural analyses based on POM, polarized IR spectroscopy, WAXRD, and molecular modeling suggested that the pendant amide groups were unidirectionally oriented and formed two sets of intramolecular hydrogen-bonding networks.
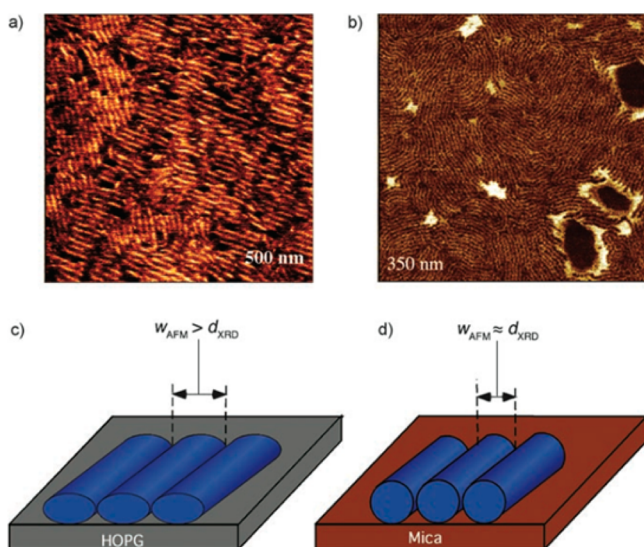
Figure 26. (a, b) AFM visualizations of poly-**47** on (a) HOPG and (b) mica. (c, d) Illustrations of cylindrical PPAs on (c) HOPG and (d) mica. The oblate shape on HOPG is due to epitaxial adsorption of the alkyl tails on the graphite underlayer. Adapted with permission from ref 102. Copyright 2006 Wiley-VCH.
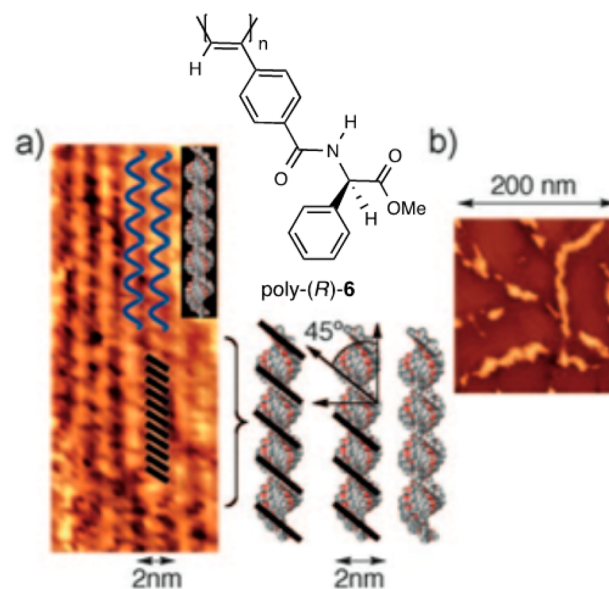

Figure 28. (a) AFM image of poly-(R)-**6** on HOPG showing single chains. (b) AFM image showing multistranded helices. Adapted with permission from ref 36. Copyright 2010 Wiley-VCH.

This arrangement generated a large electric dipole moment along the main-chain helical axis that interacted with the external electric field.

In addition to the self-assembly processes described above that lead to LCs, other PPAs have been found to form oriented films and columnar structures. These are described in the following paragraphs.

A nonchiral cis−transoid polymer synthesized by Tabata and co-workers,[126] namely, poly[(p-3-methylbutoxy)-phenylacetylene] (poly-**65**) (Figure 39), was one of the first PPAs in which a pseudohexagonal columnar structure was identified by WAXRD. It could be observed that the formation of the columnar structure was related to changes in the UV−vis spectrum of the polymer (i.e., from a yellow color in the amorphous powder to orange/red in the columnar state). Interestingly, the columnar structure could be destroyed by compression (i.e., 100 kg/cm²) to produce a trans−transoid backbone.

More recently, related studies of thermally induced crystal changes performed on poly[(p-n-heptyl)phenylacetylene] (poly-**66**) (Figure 39)[127] and poly(phenylacetylene) (poly-**21**) (Figure 14)[128] allowed relationships among different columnar structures (i.e., hexagonal, tetragonal), color changes,

and contracted cis−cisoid/stretched cis−transoid helices to be established.

It is well-known that if a polymer contains dendrons as pendants, they can enforce a helical conformation of the backbone and generate a nanoscale cylindrical object.[26] In a study of thermoreversible cis−cisoidal to cis−transoidal isomerization of helical dendronized poly(phenylacetylene)s carried out by Percec et al.,[129] a library of cis−transoidal PPAs jacketed with amphiphilic self-assembling dendrons was prepared (poly-**67** to poly-**71** and poly-**47**; Figure 40a). The resulting cylindrical PPAs self-organized into hexagonal columnar lattices with (Φ_h^{io}) and without (Φ_h) intracolumnar order, some exhibiting a hexagonal columnar crystal phase $(\Phi_{h,k})$. The reversible phase transitions observed were analyzed by a combination of differential scanning calorimetry (DSC) and small- and wide-angle XRD experiments performed on powders and oriented fibers.

Another dendronized polymer possessing a stereocenter close to the polyene backbone (poly-**72**; Figure 40b) also self-organized into a hexagonal columnar lattice with internal order (Φ_h^{io}) and a hexagonal columnar liquid-crystalline lattice (Φ_h).[130] XRD experiments revealed that the helical polymer underwent thermoreversible stretching and compression (i.e.,
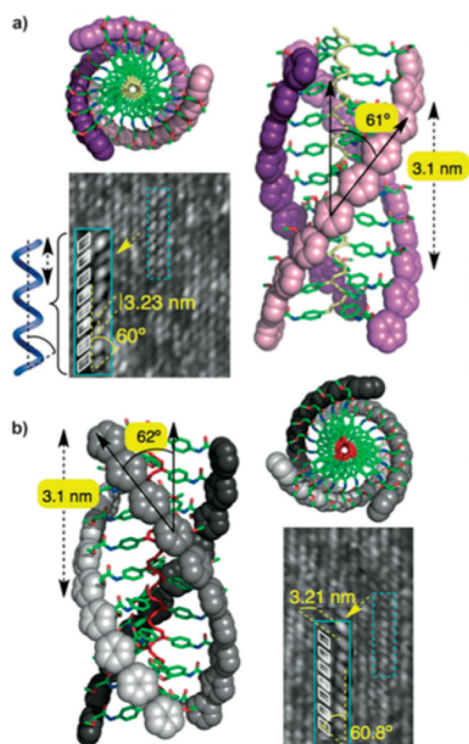

Figure 27. High-resolution AFM phase images of (a) a single layer of poly-**47** spin-cast on HOPG and (b, c) the same layer after annealing for 1 h at (b) 50 °C and (c) 100 °C. Adapted from ref 103. Copyright 2006 American Chemical Society.

Figure 29. AFM image and top and side views of (a) the 3/1 right-handed helix of poly-**22**/Ba^{2+} and (b) the 3/1 left-handed helix of poly-**22**/Ag$^+$. Adapted with permission from ref 87. Copyright 2011 Wiley-VCH.

Figure 31. AFM image and helical structure adopted by poly(**22**$_{0.6}$-*co*-**23**$_{0.4}$) after the addition of Ba(ClO$_4$)$_2$ in CHCl$_3$. Adapted with permission from ref 90. Copyright 2014 The Royal Society of Chemistry.

cis–cisoidal to cis–transoidal isomerization) during thermal cycling.

A comparison of dendronized polyacetylenes without and with a chiral center (poly-**62** and poly-**63**, respectively) by the same group revealed steric communication of chiral information.[131] These macromolecules adopt, in a reversible way, a 3D centered rectangular lattice ($\Phi_{r-c,k}$) at lower temperatures and a 2D Φ_h lattice at higher temperatures. It was found that the polymer bearing the chiral center has a larger average column stratum thickness (l). This value is related to the adoption by the PPA of a single–handed helical structure and shows how the chiral information at the periphery is transmitted to the polymer backbone through a distortion of the helical structure relative to its corresponding achiral polymer.
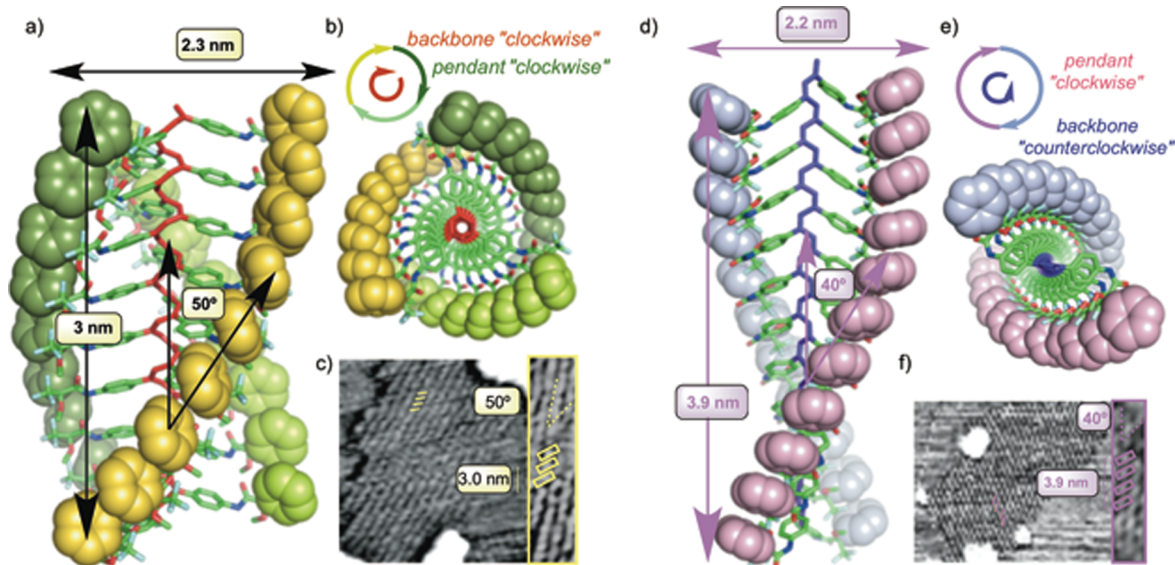
Figure 30. (a–c) Helical structure of poly-(*R*)-**1** in CHCl$_3$ obtained from molecular mechanics (MM) calculations and AFM studies: (a) side view; (b) top view; (c) AFM image after spin-casting on HOPG. (d–f) Helical structure of poly-(*R*)-**1** in THF obtained from MM calculations and AFM studies: (d) side view; (e) top view; (f) AFM image after spin-casting on HOPG. Adapted with permission from ref 32. Copyright 2013 The Royal Society of Chemistry.
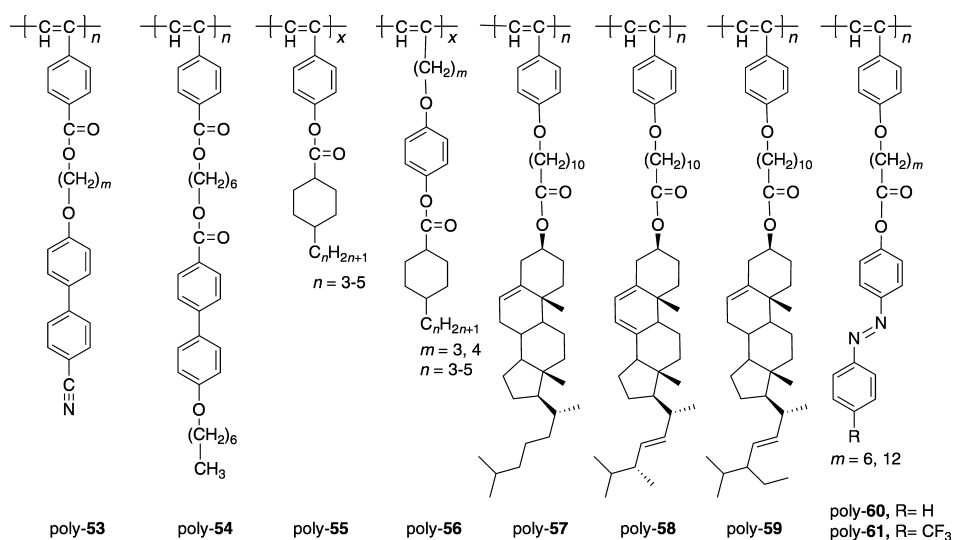
Figure 32. Different polymers presenting mesogenic pendants and liquid-crystalline properties (from poly-**53** to poly-**61**).[109−118]
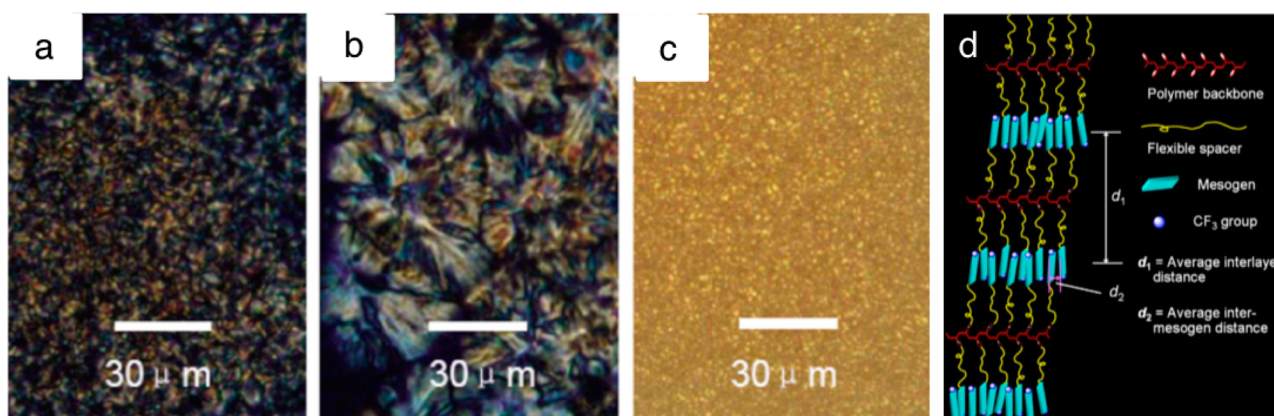

Figure 33. (a−c) Mesomorphic textures observed upon (a) cooling of poly-**60**(12) to 91.7 °C, (b) cooling of poly-**61**(12) to 91.7 °C followed by annealing for 30 min, and (c) cooling of poly-**60**(12) to 74.5 °C. The polymers were cooled from their isotropic states at a cooling rate of 3 °C/min. (d) Schematic representation of the smectic A structure of poly-**61**(12). Adapted with permission from ref 116. Copyright 2011 Elsevier Ltd.
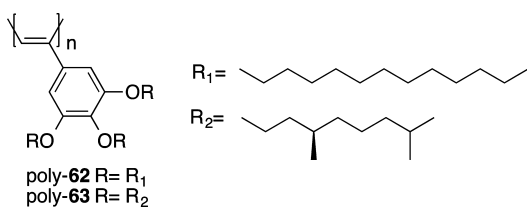
Figure 34. Structures of poly-**62** and poly-**63**.[120]

Substitution of the phenyl ring of dendronized PPAs with a 1-naphthyl ring yielded poly(1-naphthylacetylene)s poly-**73** and poly-**74** (Figure 40c),[132] which self-organized into a rectangular columnar (Φ_{r-c}) lattice, suggesting that the poly(1-naphthylacetylene)s possess greater correlation of stacking. The results also suggested that the naphthyl moiety might be better suited for expressing helical chirality in monolayer domains.

In a recent study, Chen, Yang, and co-workers synthesized PPAs that combine in the pendant fragment different mesogens with several dendronized end groups (poly-**75** to poly-**79**; Figure 41).[133] They observed that this family of polymers can self-assemble into smectic and columnar phases as a result of the coexistence of a rigid part and a flexible part in the polymer. The columnar phase is formed by a bundle of helical chains,

where the number of helices forming the bundle depends on the size of the rigid component of the polymer. It was observed that when the volume fraction of the rigid component decreases, the number of helices forming the bundle gets reduced.

A quite interesting example of how changes produced in the helical parameters of a PPA chain can be transmitted to the aggregated fibers was presented by Percec et al.[134] in a paper describing a poly(phenylacetylene) with gallic acid dendrons as pendants (Figure 42a). When this polymer is extruded, fibers of a self-organizable dendronized PPA are observed that can work as a nanomachine expressing its motion into the large length scale.[26,134−136] The backbone of this PPA presents a cis−cisoidal configuration at 25 °C, but when the fiber is warmed to 80 °C, the helical backbone isomerizes to a cis−transoidal configuration of the double bonds (Figure 42b). This process entails stretching of the helical backbone and therefore of the macroscopic fibers. The force exerted at the ends of the fiber is sufficient to mechanically displace an object with up to 250 times its mass (Figure 42c).
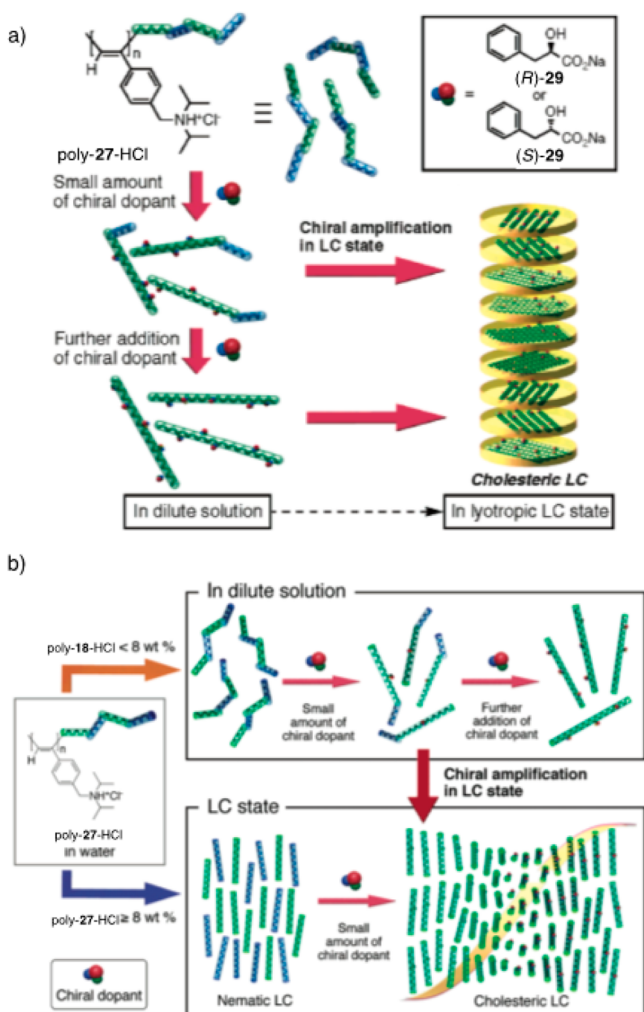
Figure 35. (a) Schematic illustration of chiral amplification of the macromolecular helicity of poly-**27**-HCl in dilute solution and the liquid-crystalline state. (b) Suggested mechanism of the hierarchical amplification process of the macromolecular helicity of poly-**27**-HCl mediated by a nonracemic dopant in dilute and concentrated water solutions. Adapted from refs 121 and 122. Copyright 2004 and 2006 American Chemical Society, respectively.

9. POLY(PHENYLACETYLENE)-BASED NANOCOMPOSITES

Efforts to convert PPAs into functional materials have also been focused on the preparation of composites and nanocomposites
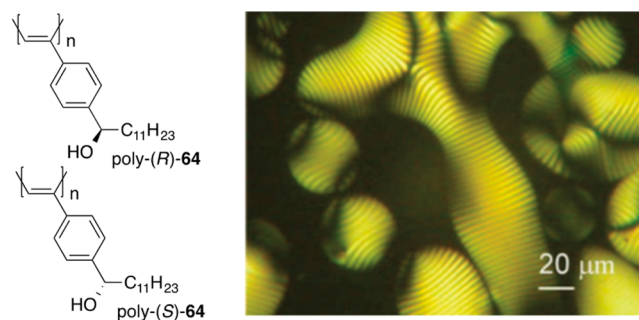
Figure 37. Structures of poly-**64** and POM image of poly-(*S*)-**64** in 20 wt % CHCl$_3$ solution. Adapted from ref 124. Copyright 2009 American Chemical Society.
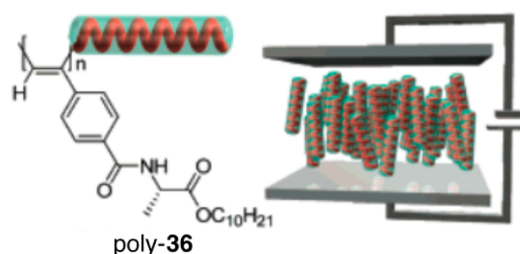
Figure 38. Schematic illustration of the electric-field-induced alignment of poly-**36** molecules. Adapted from ref 125. Copyright 2008 American Chemical Society.
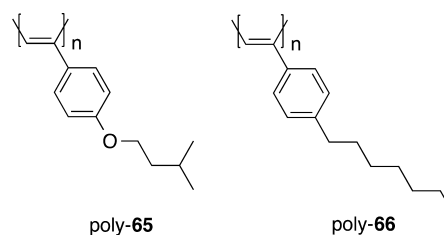

Figure 39. Structures of poly-**65** and poly-**66**.[126,127]

in which these polymers are combined with different organic or inorganic materials. In this section we will show results from the past few years on hybrid materials prepared by functionalization with PPAs of nanorods, nanoparticles, and carbon-based organic materials such as fullerenes and carbon nanotubes (CNTs).

A useful strategy to functionalize CdS nanorods with a PPA was developed by Tang and co-workers. The method involves
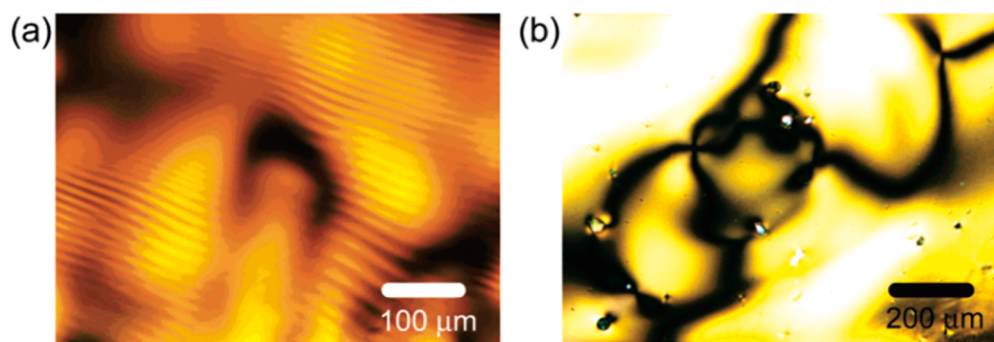

Figure 36. Polarized optical micrographs of (a) poly-**36** and (b) poly(**36**$_{0.5}$-*co*-**35**$_{0.5}$) in 15 wt % 1,2-dichloroethane solution taken at ambient temperature (20−25 °C). Adapted from ref 100. Copyright 2005 American Chemical Society.
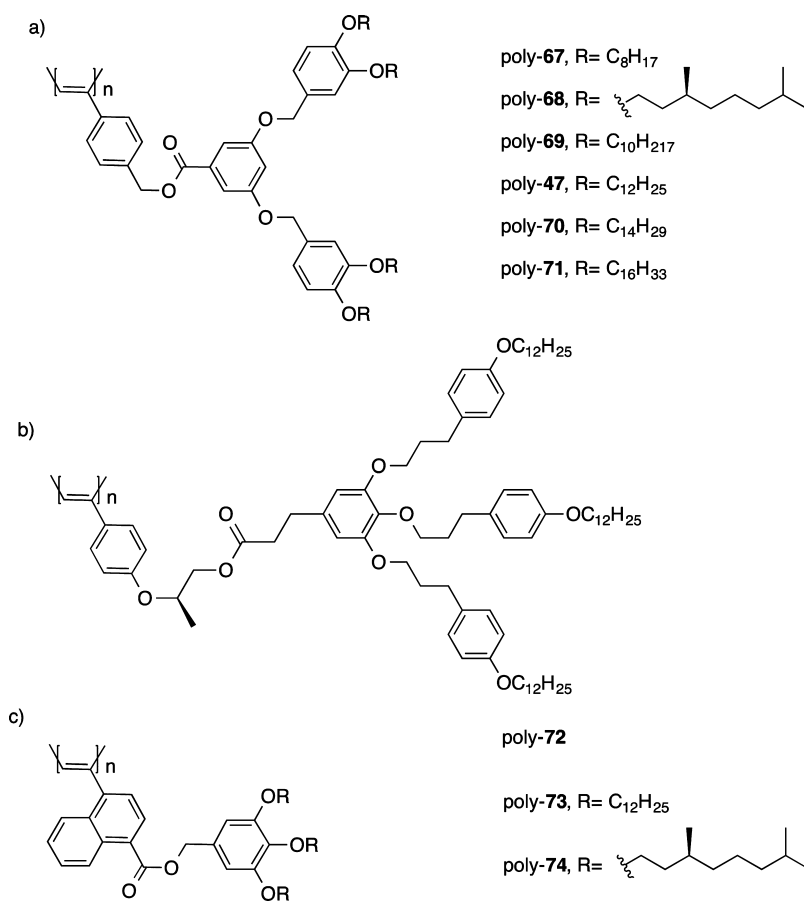
a)

poly-**67**, R= C$_8$H$_{17}$

poly-**68**, R=

poly-**69**, R= C$_{10}$H$_{217}$

poly-**47**, R= C$_{12}$H$_{25}$

poly-**70**, R= C$_{14}$H$_{29}$

poly-**71**, R= C$_{16}$H$_{33}$

b)

poly-**72**

c)

poly-**73**, R= C$_{12}$H$_{25}$

poly-**74**, R=

Figure 40. Structures of dendronized poly(phenylacetylene)s poly-**47** and poly-**67** to poly-**74** prepared by Percec et al.[129−131]

poly-**75**

poly-**76**

poly-**77**
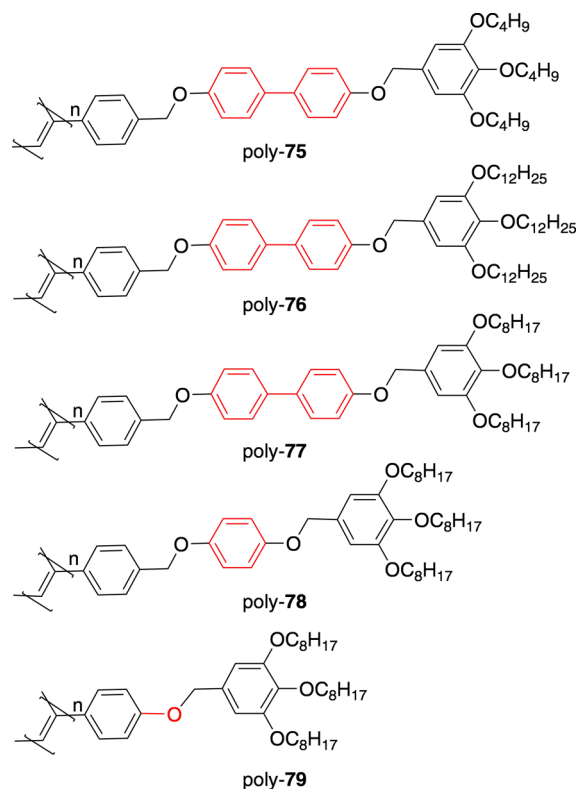
poly-**78**

poly-**79**

Figure 41. Structures of dendronized poly(phenylacetylene)s poly-**75** to poly-**79** prepared by Chen, Yang, and co-workers.[133]

polymerization of phenylacetylene (PA) monomers previously assembled on the CdS nanorod through thiol groups. It is important to note that the hybrid material could not be obtained by direct incorporation of the polymer into the CdS nanorods because of the toxicity effect of the mercapto group on the Mo, W, Ta, and Nb catalysts employed for the polymerization. In addition, when [Rh(cod)Cl]$_2$ was used as the catalyst, only insoluble products were formed, probably because of physical cross-linking between the thiol groups on the pendants. Therefore, this hybrid material was only available by anchoring the monomer to the nanorod in a first step followed by polymerization of the particles in the presence of PA monomer (Figure 43). The resulting composite is soluble in many organic solvents, including DCM, THF, and CHCl$_3$.[137]

A different approach was used by the same group to decorate ZnO nanoparticles with a PPA.[138] In this case, they prepared the polymer first and had no problems in anchoring it to the ZnO nanoparticle. To avoid physical cross-linking between the thiol groups in the chains, these groups were capped with an acetyl group (poly-**81**) or an alkyl group (poly-**82**) (Figure 44a). Hybridization between the PPA and the ZnO nano-particles was carried out by mixing the two components in CHCl$_3$, THF, or DMF. In all cases, a homogeneous suspension was formed as a result of the attractive interaction between the mercapto group of poly-**81** and the ZnO particles. This procedure looks promising for the generation of materials with optoelectronic properties. During this work, the authors also found that these polymers can also self-organize to form nanospheres, nanosheets, or nanotubes (Figure 44b−e).
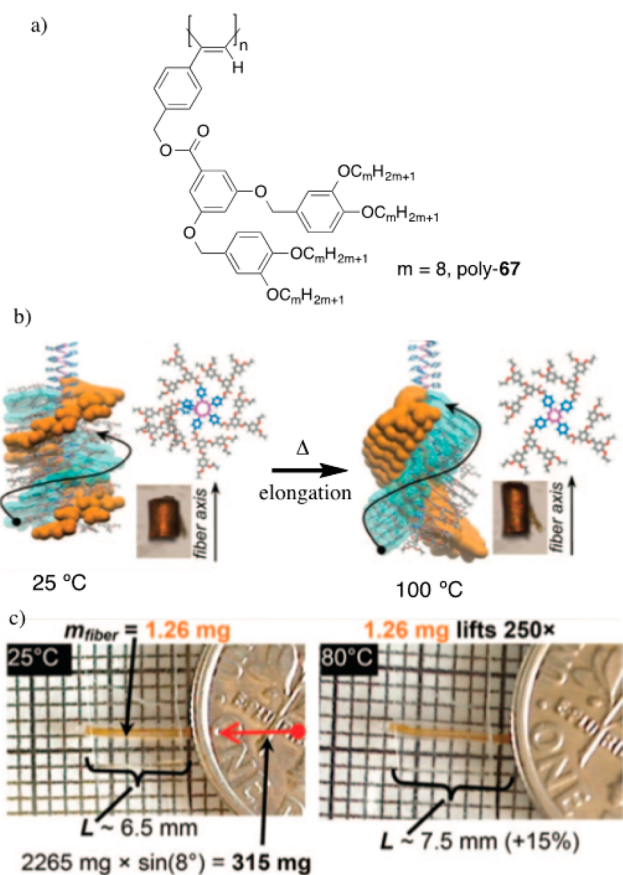
a)

b)

Δ
elongation

25 °C   100 °C

c)

m_{fiber} = 1.26 mg   1.26 mg lifts 250×

25°C   80°C

L ~ 6.5 mm   L ~ 7.5 mm (+15%)

2265 mg × sin(8°) = 315 mg

Figure 42. (a) Structure of dendronized PPA poly-**67**. (b) Stretching of the helical structure of poly-**67** by thermal isomerization of the conjugated double bonds. (c) Nanomechanical work produced by a poly-**67** fiber during its thermal expansion. Adapted from ref 134. Copyright 2008 American Chemical Society.

Fullerenes and CNTs are carbon allotropes with important mechanical, thermal, electronic, and optical properties that provide a broad range of applications. The combination of
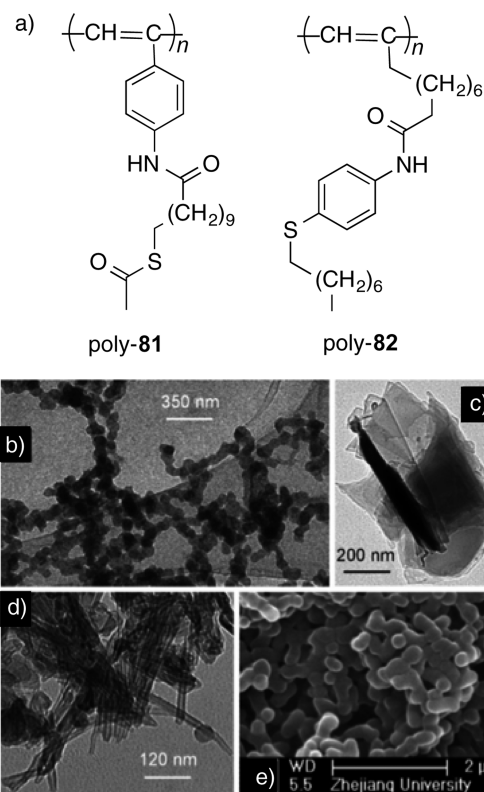
a)

poly-**81**   poly-**82**

b)

c)

d)

e)

Figure 44. (a) Structures of PPAs poly-**81** and poly-**82**. (b–d) TEM images of (b) nanoparticles, (c) nanosheets, and (d) nanotubes of poly-**81**. (e) SEM image of poly-**81** nanoparticles. Adapted from ref 138. Copyright 2008 American Chemical Society.

these materials with polymers has attracted the attention of some research groups interested in the generation of composites with applications in biological and material sciences.

Within the field of PPAs, Yashima and co-workers prepared helical PPAs bearing C_{60} fullerenes oriented in a one-handed helical array. The introduction of the fullerenes into the helical polymer was carried out by copolymerization of an achiral C_{60}-
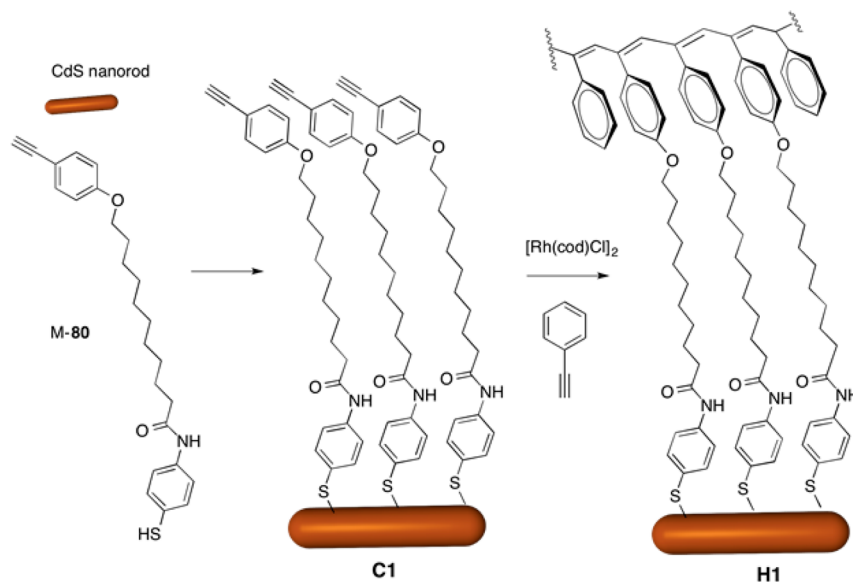

Figure 43. Assembly of monomers M-**80** on the surface of the CdS nanorod to yield composite C1, which after polymerization in the presence of polyacetylene monomer gives the hybrid material H1.[137]
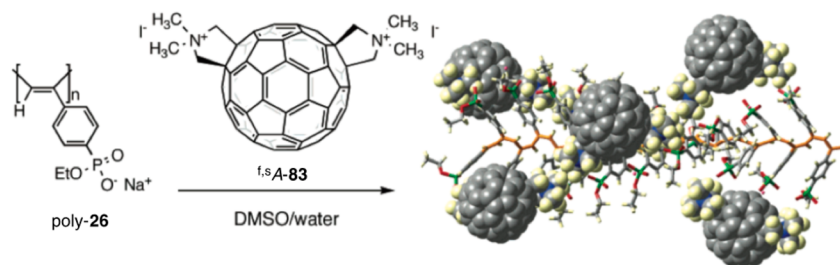
Figure 45. Schematic representation of macromolecular helicity induction in poly-**26** using the optically active fullerene $^{f,s}A$-**83**. Adapted from ref 140. Copyright 2004 American Chemical Society.

bound phenylacetylene with a chiral phenylacetylene.[94] In this case, the polymerization gave a composite in which the fullerenes are oriented in a one-handed helical array. In a different experiment, the achiral C_{60}-bound phenylacetylene was polymerized with an achiral phenylacetylene, yielding a composite that required the addition of a chiral external stimulus to get a single helical sense.[139]

In a different approach to prepare PPAs with the fullerenes oriented in a one-handed helical array, Yashima and co-workers explored the use of supramolecular cation−anion interactions to bind the fullerenes to the helical PPA.[140] They selected as the anionic component an achiral PPA carrying monoethyl phosphonates (poly-**26**), which was combined with a cationic C_{60} bisadduct whose chirality was used to induce a specific helical sense in the optically inactive PPA (Figure 45).

Tang and co-workers developed a different methodology to functionalize a fullerene with a PPA. This consisted of the preparation of a mixture of C_{60} and the phenylacetylene in the
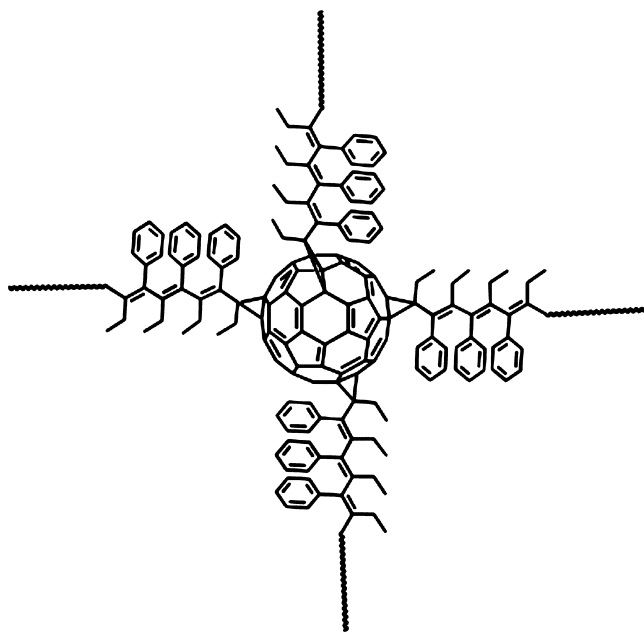

Figure 46. Functionalization of C_{60} with substituted polyacetylenes.[141]

presence of a tungsten catalyst, yielding C_{60}-containing polyacetylenes with high molecular weights in high yields. It is worth noting that in this case, the PPA is linked to C_{60} through the polyene backbone and not through the pendant groups as in most of the other examples (Figure 46).[141]

One of the main limitations of CNTs for the preparation of devices with electronic or optical properties is their very low

solubility, which makes them almost intractable. During the past decade different groups have studied ways to improve their solubility in organic solvents and water. The common approach has involved non-covalent functionalization of the CNTs with conjugated polymers to produce soluble hybrid materials that conserve the properties of the CNTs. All of the aspects related to the functionalization and properties of CNT/PPA hybrid materials have been the subject of a recent review,[142] and therefore, we focus here on the formation of the hybrid materials by supramolecular interactions.

The pioneer work in this field was carried out by Tang and Xu,[143] who solubilized the CNTs by in situ polymerization of phenylacetylene monomer in the presence of the CNTs. In a second approach, Tang and co-workers found that the introduction of fused rings (e.g., pyrene) as pendant groups of the PPA increased the solubility of the CNTs as a result of the better interaction between the PPA and the CNTs.[144] They also observed that the solubility of the polymer is directly related to the degree of solubilization of the CNTs. Thus, while poly-**86** is almost insoluble in THF and presents a null effect on the dispersion of CNTs in THF, poly-**87** is highly soluble in THF and presents the highest solvating power toward CNTs among all of the pyrene PPA derivatives (poly-**84** to poly-**88** and poly-**93** to poly-**94**; Figure 47). The solvating power of pyrene−PPA derivatives is much higher than that observed for a pyrene-functionalized polystyrene,[145] indicating the important role of the extended conjugation in the dispersion of CNTs. The same group compared the solvating powers of the PPA poly-**84** (575 mg/mL) and its polyacetylene analogue poly-**88** (467 mg/mL) in THF and deduced that the presence of the phenyl ring close to the backbone of the polymer favors the dispersion of the CNTs.[146] These results were further confirmed on PPAs bearing different aromatic systems as the pendant moieties (poly-**89** to poly-**96**; Figure 47).[147−150]

When the pendants of the PPA contain polar or ionizable groups (e.g., carboxyl or amino groups; Figure 48), the resulting PPA polyelectrolytes can be used to dissolve multiwalled carbon nanotubes (MWCNTs) in water, reaching concentrations as high as 300 mg/L, by the formation of PPA/MWCNT nanohybrids[151,152] (Figure 49). Moreover, these hybrids have been decorated with nanoparticles of different metals, yielding multicomponent PPA electrolyte/MWCNT/nanoparticle composites (Figure 50).[151,152]

Interestingly, this strategy to improve the water solubility of MWCNTs did not work so well when sugar-containing PPAs were used.[153] In this case, the polymerization of a monosaccharide-substituted phenylacetylene in the presence of the MWCNT generated a water-soluble composite, but it contained only around 2 wt % MWCNTs. The authors explained this low loading as originating during the polymer-
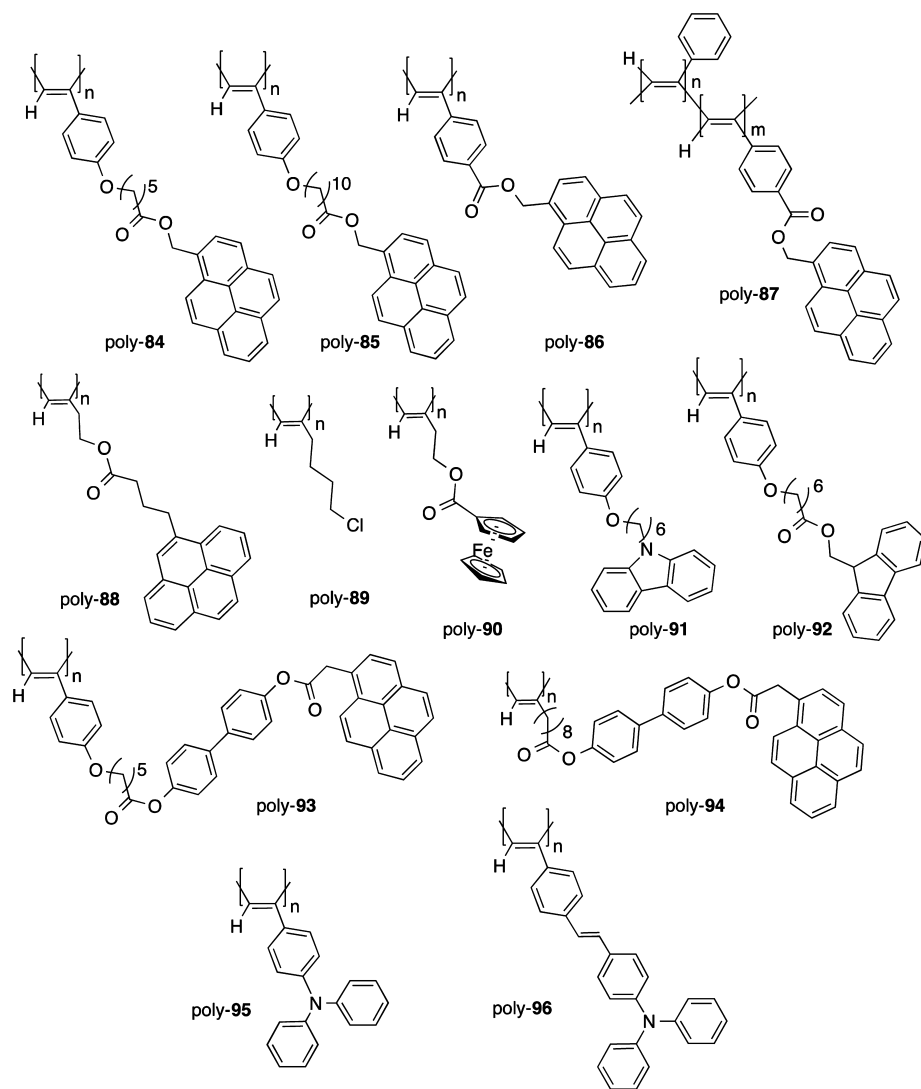
Figure 47. PPA derivatives used to disperse CNTs in organic solvents.[143−150]
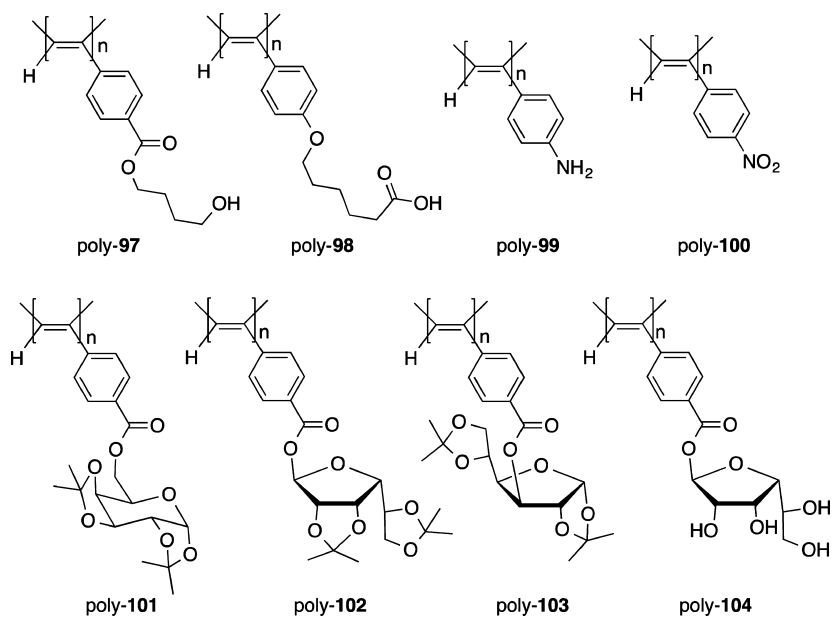

Figure 48. PPA derivatives with polar groups used to disperse CNTs in water.[151,152]
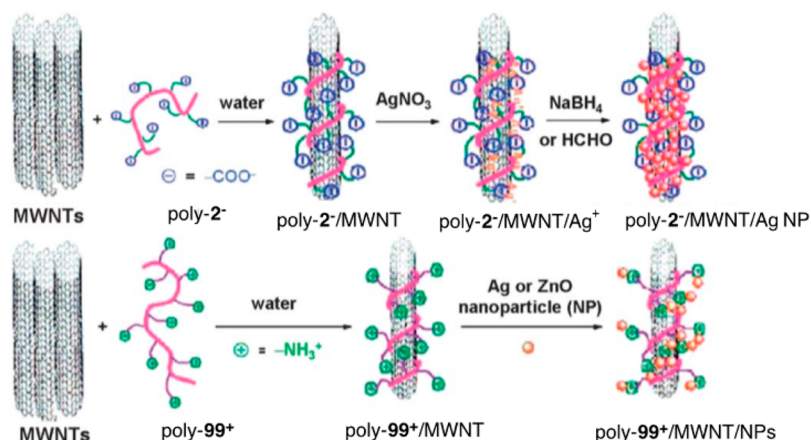
Figure 49. Scheme showing the dispersion of CNTs from aggregates to single tubes by wrapping them with the polyelectrolytes poly-2⁻ and poly-99⁺ and the subsequent interactions with Ag or ZnO nanoparticles. Reproduced from ref 151. Copyright 2008 American Chemical Society.
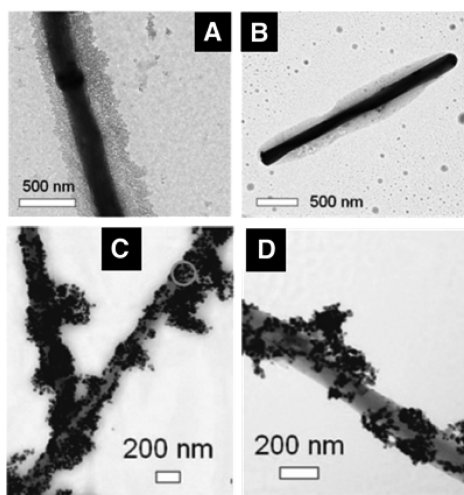

Figure 50. TEM images of (A) poly-2⁻/MWCNT and (B) poly-99⁺/MWCNT and their corresponding silver nanohybrids (C) poly-2⁻/MWCNT/Ag (prepared using NaBH₄ as the reductant) and (D) poly-99⁺/MWCNT/Ag. Adapted from ref 151. Copyright 2008 American Chemical Society.

ization process. At the beginning, $\pi-\pi$ interactions between the hydrophobic part of the PPA chain and the MWCNT take place, solubilizing the polymer, but once the polymer chain has grown, the bulkiness of the monosaccharides impedes those interactions, limiting the solubility of the MWCNT.

Apart from MWCNTs, single-walled carbon nanotubes (SWCNTs) have also been the object of solubility improvements using similar approaches. The groups of Yang and Chen used PPAs to make hybrids with SWCNTs having improved solubility in organic solvents.[154] In their experiments, dendronized PPAs bearing 3,4,5-tris(octyloxy)phenyl pendant groups linked to the PPA backbone with different spacers were tested, and the results showed that while the formation of the composite was improved by the presence of aryl rings in the pendants because of $\pi-\pi$ interactions between the PPA and the SWCNT, the presence of long alkyl chains at the end of the pendants prevented aggregation (Figure 51).

10. CONCLUSIONS

In the last two decades, PPAs have shown their great potential to generate a variety of supramolecular assemblies such as fibers, nanospheres, hybrid materials, liquid crystals, sterocomplexes, etc., that combine the geometrical and chiroptical properties associated with the helical character of the PPAs with those provided by the large, structurally diverse functions attached to the polyene backbone as pendants. The combination of those two factors has produced a miscellany of novel assemblies based on interchain interactions, mainly through hydrogen bonds and hydrophobic and electrostatic forces. Ligands for metal complexation, mesogenic groups for liquid crystallinity, and carbon nanotubes are only a few examples of groups and species that have been incorporated to the PPAs to generate supramolecular assemblies and hybrid materials with new properties of interest.

The importance of PPAs as starting units for new assemblies comes from their (a) tunable helical structure, (b) great variety of functional groups that can be introduced as pendants in a PPA polymer or copolymer chain, and (c) the encapsulating ability of the assemblies. These properties, together with the results already obtained and reported in this review, suggest the great potential of PPA-derived aggregates in directions not very much explored to date. Thus, macroscopically chiral assemblies with helicities tunable by external stimuli and endowed with some additional functionality could offer approaches to new and tunable asymmetric catalysts,[155−159] nanoreactors,[160] chiral recognition agents,[161] and chiral stationary phases,[162,163] among others.[25]

A second aspect that may deserve interest relates to biomedical applications. The great majority of the papers on PPAs have focused on new materials, sensors, etc., and only a very few have focused on biomedical and related fields.[35,164] Naturally, biocompatibility, toxicity, and water solubility issues have to be solved, but the advantages of combining stimuli-responsive supramolecular aggregation with chirality control and/or recognition and encapsulation may deserve a try. Also, further developments in the transformation of chemical interactions into mechanical energy as in fibers[134] could constitute good models for artificial muscles.

Finally, the supramolecular assemblies formed from PPAs with short pendants frequently show poor AFM images that do not allow visualization of the angle, pitch, and type of package of the helical components. This limitation comes from the low quality of the 2D layer and precludes the study of the transference of helicity from solution to the solid state. We
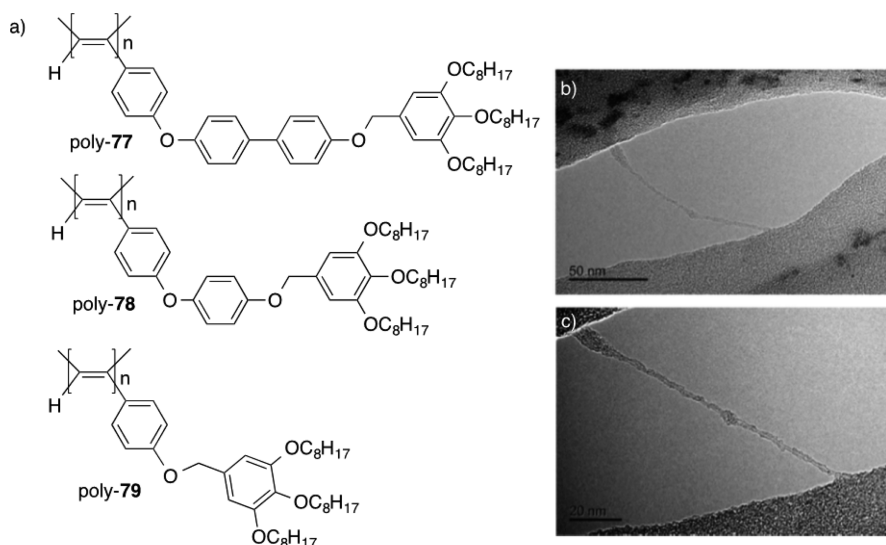
Figure 51. (a) Structure of poly-77 to poly-79. (b, c) TEM images indicating the presence of individual polymer/SWCNT fibrils at different magnifications: (b) 50 nm and (c) 20 nm. Adapted from ref 154. Copyright 2013 American Chemical Society.

believe that efforts on new deposition methods to obtain high-resolution AFM images deserve to be explored.

We hope that this review will stimulate researchers to further explore the formation and properties of supramolecular assemblies derived from PPAs.

AUTHOR INFORMATION

Corresponding Author

*E-mail: ricardo.riguera@usc.es.

Notes

The authors declare no competing financial interest.

Biographies

Félix Freire obtained his B.Sc. (2000), M.Sc. (2002), and Ph.D. (2005) in Chemistry from the University of Santiago de Compostela (USC). In 2005 he did a postdoctoral stay in the group of Prof. Jesús Jiménez Barbero at CSIC-Madrid, where he worked on NMR studies of biomolecules. During 2006−2008 he was a Fulbright Postdoctoral Fellow in the group of Samuel H. Gellman, studying the folding of parallel β-sheets in water, and since 2009 he has worked at the University of Santiago as a Ramón y Cajal Researcher. His research interests include stimuli-responsive polymers, polymer self-assembly, and chiral polymer particles.

Emilio Quiñoá obtained his Ph.D. in Chemistry at the University of Santiago de Compostela in the subject of bioactive marine natural products. After postdoctoral research at the University of California at Santa Cruz, he became an Associate Professor (1989) and later a Full Professor of Organic Chemistry (1998). His research addressed the development of methods for the assignment of absolute configuration by NMR spectroscopy. He has coauthored more than 100 scientific publications and a number of textbooks and patent applications and has received several research awards. In 2010 he joined the Center for Research in Biological Chemistry and Molecular Materials (CIQUS) at USC. His current research interests are focused on the study of dynamic helical polymers and their applications in nanotechnology.

Prof. Ricardo Riguera is Full Professor of Organic Chemistry at the Universidad de Santiago de Compostela (Spain). His research has covered bioactive natural products, medicinal chemistry, and NMR methods for the determination of absolute configuration. In the past few years he has become interested in polymeric nanostructures for biomedical applications and in stimuli-responsive dynamic polymers. In regard to academic posts, he has been the Director of the Department, the Dean of the Faculty of Chemistry, and Vice Chancellor of the University. In 2013 he was awarded the Félix Serratosa Medal by the Real Sociedad Española de Química.

REFERENCES

(1) *Hierarchical Macromolecular Structures: 60 Years after the Staudinger Nobel Prize I*; Percec, V., Ed.; Advances in Polymer Science, Vol. *261*; Springer: New York, 2013.

(2) *Hierarchical Macromolecular Structures: 60 Years after the Staudinger Nobel Prize II*; Percec, V., Ed.; Advances in Polymer Science, Vol. *262*; Springer: New York, 2013.

(3) Lehn, J.-M. *Supramolecular Chemistry: Concepts and Perspectives*; Wiley-VCH: Weinheim, Germany, 1995.

(4) Steed, J. W.; Atwood, J. L. *Supramolecular Chemistry*; John Wiley & Sons: West Sussex, U.K., 2009.

(5) Cragg, P. J. *A Practical Guide to Supramolecular Chemistry*; John Wiley & Sons: West Sussex, U.K., 2005.

(6) Duan, P.; Cao, H.; Zhang, L.; Liu, M. Gelation Induced Supramolecular Chirality: Chirality Transfer, Amplification and Application. *Soft Matter* 2014, *10*, 5428−5448.

(7) Zhang, L.; Qin, L.; Wang, X.; Cao, H.; Liu, M. Supramolecular Chirality in Self-Assembled Soft Materials: Regulation of Chiral Nanostructures and Chiral Functions. *Adv. Mater.* 2014, *26*, 6959−6964.

(8) Yang, Y.; Zhang, Y.; Wei, Z. Supramolecular Helices: Chirality Transfer from Conjugated Molecules to Structures. *Adv. Mater.* 2013, *25*, 6039−6049.

(9) Wang, Y.; Xu, J.; Wang, Y.; Chen, H. Emerging Chirality in Nanoscience. *Chem. Soc. Rev.* 2013, *42*, 2930−2962.

(10) Miyake, H.; Tsukube, H. Coordination Chemistry Strategies for Dynamic Helicates: Time-programmable Chirality Switching with Labile and Inert Metal Helicates. *Chem. Soc. Rev.* 2012, *41*, 6977−6991.

(11) Smith, D. K. Lost in Translation? Chirality Effects in the Self-Assembly of Nanostructured Gel-phase Materials. *Chem. Soc. Rev.* 2009, *38*, 684−694.

(12) Praveen, V. K.; Babu, S. S.; Vijayakumar, C.; Varghese, R.; Ajayaghosh, A. Helical Supramolecular Architectures of Self-Assembled Linear π-Systems. *Bull. Chem. Soc. Jpn.* 2008, *81*, 1196−1211.

(13) Palmans, A. R. A.; Meijer, E. W. Amplification of Chirality in Dynamic Supramolecular Aggregates. *Angew. Chem., Int. Ed.* 2007, *46*, 8948−8968; *Angew. Chem.* 2007, *119*, 9106−9126.

(14) Mateos-Timoneda, M. A.; Crego-Calama, M.; Reinhoudt, D. N. Supramolecular Chirality of Self-Assembled Systems in Solution. *Chem. Soc. Rev.* 2004, *33*, 363−37.

(15) Li, A. D. Q. *Molecular Self-Assembly: Advances and Applications*; CRC Press: Boca Raton, FL, 2013.

(16) Loh, X. J.; Scherman, O. A. *Polymeric and Self Assembled Hydrogels*; The Royal Society of Chemistry: Cambridge, U.K., 2013.

(17) Harada, A. *Supramolecular Polymer Chemistry*; Wiley-VCH: Weinheim, Germany, 2012.

(18) Hadjichristidis, N.; Hirao, A.; Tezuka, Y.; Prez, F. D. *Complex Macromolecular Architectures*; John Wiley & Sons (Asia): Singapore, 2011.

(19) Hao, J. *Self-Assembled Structures: Properties and Applications in Solution and on Surfaces*; CRC Press: Boca Raton, FL, 2010.

(20) Geckeler, K. E.; Nishide, H. *Advanced Nanomaterials*; Wiley-VCH: Weinheim, Germany, 2010; Vols. *1 and 2*.

(21) Ozin, G. A.; Arsenault, A. C.; Cadermatiri, L. *Nanochemistry: A Chemical Approach to Nanomaterials*; The Royal Society of Chemistry: Cambridge, U.K., 2010.

(22) Lee, Y. S. *Self-Assembly and Nanotechnology: A Force Balance Approach*; John Wiley & Sons: Hoboken, NJ, 2008.

(23) Rotello, V. M.; Thayumanavan, S. *Molecular Recognition and Polymers*; John Wiley & Sons: Hoboken, NJ, 2008.

(24) Kickelbick, G. *Hybrid Materials: Synthesis, Characterization, and Applications*; Wiley-VCH: Weinheim, Germany, 2007.

(25) Yashima, E.; Maeda, K.; Iida, H.; Furusho, Y.; Nagai, K. Helical Polymers: Synthesis, Structures, and Functions. *Chem. Rev.* 2009, *109*, 6102−6211.

(26) Liu, J.; Lam, J. W. Y.; Tang, B. Z. Acetylenic Polymers: Syntheses, Structures, and Functions. *Chem. Rev.* 2009, *109*, 5799−5867.

(27) Rosen, B. M.; Wilson, C. J.; Wilson, D. A.; Peterca, M.; Imam, M. R.; Percec, V. Dendron-Mediated Self-Assembly, Disassembly, and Self-Organization of Complex Systems. *Chem. Rev.* 2009, *109*, 6275−6540.

(28) Yashima, E.; Maeda, K.; Furusho, Y. Functional Polyacetylenes. *Acc. Chem. Res.* 2008, *41*, 1166−1180.

(29) Rudick, J. G.; Percec, V. Induced Helical Backbone Conformations of Self-Organizable Dendronized Polymers. *Acc. Chem. Res.* 2008, *41*, 1641−1652.

(30) Yashima, E.; Maeda, K. Chirality-Responsive Helical Polymers. *Macromolecules* 2008, *41*, 3−12.

(31) Lam, J. W. Y.; Tang, B. Z. Functional Polyacetylenes. *Acc. Chem. Res.* 2005, *38*, 745−754.

(32) Leiras, S.; Freire, F.; Seco, J. M.; Quiñoá, E.; Riguera, R. Controlled Modulation of the Helical Sense and the Elongation of Poly(phenylacetylene)s by Polar and Donor Effects. *Chem. Sci.* 2013, *4*, 2735−2743.

(33) Hu, Y.; Liu, R.; Sanda, F.; Masuda, T. Synthesis of Glutamic Acid-based Dendritic Helical Poly(phenylacetylene)s. *Polym. J.* 2008, *40*, 143−147.

(34) Sakurai, S.; Okoshi, K.; Kumaki, J.; Yashima, E. Two-Dimensional Surface Chirality Control by Solvent-Induced Helicity Inversion of a Helical Polyacetylene on Graphite. *J. Am. Chem. Soc.* 2006, *128*, 5650−5651.

(35) Cheuk, K. K. L.; Li, B. S.; Lam, J. W. Y.; Xie, Y.; Tang, B. Z. Synthesis, Chain Helicity, Assembling Structure, and Biological Compatibility of Poly(phenylacetylene)s Containing L-Alanine Moieties. *Macromolecules* 2008, *41*, 5997−6005.

(36) Louzao, I.; Seco, J. M.; Quiñoá, E.; Riguera, R. Control of the Helicity of Poly(phenylacetylene)s: From the Conformation of the Pendant to the Chirality of the Backbone. *Angew. Chem., Int. Ed.* 2010, *49*, 1430−1433.

(37) Yashima, E.; Maeda, K.; Sato, O. Switching of a Macromolecular Helicity for Visual Distinction of Molecular Recognition Events. *J. Am. Chem. Soc.* 2001, *123*, 8159−8160.

(38) Maeda, K.; Kamiya, N.; Yashima, E. Poly(phenylacetylene)s Bearing a Peptide Pendant: Helical Conformational Changes of the Polymer Backbone Stimulated by the Pendant Conformational Change. *Chem. - Eur. J.* 2004, *10*, 4000−4010.

(39) Zhao, H. C.; Sanda, F.; Masuda, T. Synthesis and Helical Conformation of Poly(N-propargylamides) Carrying L-Aspartic Acid in the Side Chain. *J. Polym. Sci., Part A: Polym. Chem.* 2005, *43*, 5168−5176.

(40) Zhao, H. C.; Sanda, F.; Masuda, T. Control of Helical Sense and Tightness of Amino Acid-Based Poly(N-propargylamide) by Temperature and Solvents. *Macromol. Chem. Phys.* 2005, *206*, 1653−1658.

(41) Sanda, F.; Terada, K.; Masuda, T. Synthesis, Chiroptical Properties, and pH Responsibility of Aspartic Acid- and Glutamic Acid-Based Helical Polyacetylenes. *Macromolecules* **2005**, *38*, 8149−8154.

(42) Maeda, K.; Mochizuki, H.; Watanabe, M.; Yashima, E. Switching of Macromolecular Helicity of Optically Active Poly(phenylacetylene)s Bearing Cyclodextrin Pendants Induced by Various External Stimuli. *J. Am. Chem. Soc.* **2006**, *128*, 7639−7650.

(43) Maeda, K.; Wakasone, Sh.; Shimomura, K.; Ikai, T.; Kanoh, Sh. Chiral Amplification in Polymer Brushes Consisting of Dynamic Helical Polymer Chains through the Long-Range Communication of Stereochemical Information. *Macromolecules* **2014**, *47*, 6540−6546.

(44) Simionescu, C. I.; Percec, V.; Dumitrescu, S. Polymerization of Acetylenic Derivatives. XXX. Isomers of Polyphenylacetylene. *J. Polym. Sci., Polym. Chem. Ed.* **1977**, *15*, 2497−2509.

(45) Simionescu, C. I.; Percec, V. Polypentadeuterophenylacetylene Isomers. *J. Polym. Sci., Polym. Lett. Ed.* **1979**, *17*, 421−429.

(46) Simionescu, C. I.; Percec, V. Thermal Cis−Trans Isomerization of Cis−Transoidal Polyphenylacetylene. *J. Polym. Sci., Polym. Chem. Ed.* **1980**, *18*, 147−155.

(47) Furlani, A.; Napoletano, C.; Russo, M. V.; Feast, W. J. Stereoregular Polyphenylacetylene. *Polym. Bull.* **1986**, *16*, 311−317.

(48) Tabata, M.; Yang, W.; Yokota, K. Polymerization of *m*-Chlorophenylacetylene Initiated by [Rh(norbornadiene)Cl]₂-Triethylamine Catalyst Containing Long-Lived Propagation Species. *Polym. J.* **1990**, *22*, 1105−1107.

(49) Kishimoto, Y.; Eckerle, P.; Miyatake, T.; Ikariya, T.; Noyori, R. Living Polymerization of Phenylacetylenes Initiated by Rh-(C.tplbond.CC₆H₅)(2,5-norbornadiene)[P(C₆H₅)₃]₂. *J. Am. Chem. Soc.* **1994**, *116*, 12131−12132.

(50) Morino, K.; Watase, N.; Maeda, K.; Yashima, E. Chiral Amplification in Macromolecular Helicity Assisted by Noncovalent Interaction with Achiral Amines and Memory of the Helical Chirality. *Chem. - Eur. J.* **2004**, *10*, 4703−4707.

(51) Maeda, K.; Morino, K.; Okamoto, Y.; Sato, T.; Yashima, E. Mechanism of Helix Induction on a Stereoregular Poly((4-carboxyphenyl)acetylene) with Chiral Amines and Memory of the Macromolecular Helicity Assisted by Interaction with Achiral Amines. *J. Am. Chem. Soc.* **2004**, *126*, 4329−4342.

(52) Maeda, K.; Hatanaka, K.; Yashima, E. Helix Induction in an Optically Inactive Poly[(4-carboxyphenyl)acetylene] Film with Chiral Amines. *Mendeleev Commun.* **2004**, *14*, 231−233.

(53) Yashima, E.; Matsushima, T.; Okamoto, Y. Poly((4-carboxyphenyl)acetylene) as a Probe for Chirality Assignment of Amines by Circular Dichroism. *J. Am. Chem. Soc.* **1995**, *117*, 11596−11597.

(54) Leiras, S.; Freire, F.; Quiñoá, E.; Riguera, R. Reversible Assembly of Enantiomeric Helical Polymers: from Fibers to Gels. *Chem. Sci.* **2015**, *6*, 246−253.

(55) Sakurai, S.-I.; Kuroyanagi, K.; Morino, K.; Kunitake, M.; Yashima, E. Atomic Force Microscopy Study of Helical Poly-(phenylacetylene)s on a Mica Substrate. *Macromolecules* **2003**, *36*, 9670−9674.

(56) Shinohara, K.; Yasuda, S.; Kato, G.; Fujita, M.; Shigekawa, H. Direct Measurement of the Chiral Quaternary Structure in a π-Conjugated Polymer at Room Temperature. *J. Am. Chem. Soc.* **2001**, *123*, 3619−3620.

(57) Li, B. S.; Lam, J. W. Y.; Yu, Z.-Q.; Tang, B. Z. Tunable Helical Assemblies of L-Alanine Methyl Ester-Containing Polyphenylacety-lene. *Langmuir* **2012**, *28*, 5770−5774.

(58) Li, B. S.; Cheuk, K. K. L.; Yang, D.; Lam, J. W. Y.; Wan, L. J.; Bai, C.; Tang, B. Z. Self-Assembling of an Amphiphilic Polyacetylene Carrying L-Leucine Pendants: A Homopolymer Case. *Macromolecules* **2003**, *36*, 5447−5450.

(59) Cheuk, K. K. L.; Lam, J. W. Y.; Chen, J.; Lai, L. M.; Tang, B. Z. Amino Acid-Containing Polyacetylenes: Synthesis, Hydrogen Bonding, Chirality Transcription, and Chain Helicity of Amphiphilic Poly(phenylacetylene)s Carrying L-Leucine Pendants. *Macromolecules* **2003**, *36*, 5947−5959.

(60) Li, B. S.; Kang, S. Z.; Cheuk, K. K. L.; Wan, L.; Ling, L.; Bai, C.; Tang, B. Z. Self-assembling of Helical Poly(Phenylacetylene) Carrying L-Valine Pendants in Solution, on Mica Substrate, and on Water Surface. *Langmuir* **2004**, *20*, 7598−7603.

(61) Li, B. S.; Cheuk, K. K. L.; Ling, L.; Chen, J.; Xiao, X.; Bai, C.; Tang, B. Z. Synthesis and Hierarchical Structures of Amphiphilic Polyphenylacetylenes Carrying L-Valine Pendants. *Macromolecules* **2003**, *36*, 77−85.

(62) Cheuk, K. K. L.; Lam, J. W. Y.; Lai, L. M.; Dong, Y.; Tang, B. Z. Syntheses, Hydrogen-Bonding Interactions, Tunable Chain Helicities, and Cooperative Supramolecular Associations and Dissociations of Poly(Phenylacetylene)s Bearing L-Valine Pendants: Toward the Development of Proteomimetic Polyenes. *Macromolecules* **2003**, *36*, 9752−9762.

(63) Li, B. S.; Cheuk, K. K. L.; Salhi, F.; Lam, J. W. Y.; Cha, J. A. K.; Xiao, X.; Bai, C.; Tang, B. Z. Tuning the Chain Helicity and Organizational Morphology of an L-Valine-Containing Polyacetylene by pH Change. *Nano Lett.* **2001**, *1*, 323−328.

(64) Li, B. S.; Chen, J.; Zhu, C. F.; Leung, K. K. L.; Wan, L.; Bai, C.; Tang, B. Z. Formation of Porous Films and Vesicular Fibers via Self-Organization of an Amphiphilic Chiral Oligomer. *Langmuir* **2004**, *20*, 2515−2518.

(65) Maeda, K.; Mochizuki, H.; Osato, K.; Yashima, E. Stimuli-Responsive Helical Poly(phenylacetylene)s Bearing Cyclodextrin Pendants that Exhibit Enantioselective Gelation in Response to Chirality of a Chiral Amine and Hierarchical Super-Structured Helix Formation. *Macromolecules* **2011**, *44*, 3217−3226.

(66) Nagai, K.; Maeda, K.; Takeyama, Y.; Sato, T.; Yashima, E. Temperature-Induced Chiroptical Changes in a Helical Poly-(phenylacetylene) Bearing *N,N*-Diisopropylaminomethyl Groups with Chiral Acids in Water. *Chem. - Asian J.* **2007**, *2*, 1314−1321.

(67) Miyagawa, T.; Yamamoto, M.; Muraki, R.; Onouchi, H.; Yashima, E. Supramolecular Helical Assembly of an Achiral Cyanine Dye in an Induced Helical Amphiphilic Poly(phenylacetylene) Interior in Water. *J. Am. Chem. Soc.* **2007**, *129*, 3676−3682.

(68) Liu, W.; Cui, Z.-M.; Liu, Q.; Yan, D.-W.; Wu, J.-Y.; Yan, H.-J.; Guo, Y.-L.; Wang, C.-R.; Song, W.-G.; Liu, Y.-Q.; Wan, L.-J. Catalytic Synthesis and Structural Characterizations of a Highly Crystalline Polyphenylacetylene Nanobelt Array. *J. Am. Chem. Soc.* **2007**, *129*, 12922−12923.

(69) Rao, J. P.; Geckeler, K. E. Polymer nanoparticles: Preparation Techniques and Size-Control Parameters. *Prog. Polym. Sci.* **2011**, *36*, 887−913.

(70) Li, W.; Huang, H.; Li, Y.; Deng, J. Particles of Polyacetylene and its Derivatives: Preparation and Applications. *Polym. Chem.* **2014**, *5*, 1107−1118.

(71) Song, C.; Liu, X.; Liu, D.; Ren, C.; Yang, W.; Deng, J. Optically Active Particles of Chiral Polymers. *Macromol. Rapid Commun.* **2013**, *34*, 1426−1445.

(72) Zhang, Y.; Luo, X.; Deng, J.; Yang, W. Preparation of Optically Active Nanoparticles by Emulsification of Preformed Helical Polymers. *Macromol. Chem. Phys.* **2011**, *212*, 353−360.

(73) Deng, J.; Chen, B.; Luo, X.; Yang, W. Synthesis of Nano-Latex Particles of Optically Active Helical Substituted Polyacetylenes via Catalytic Microemulsion Polymerization in Aqueous Systems. *Macromolecules* **2009**, *42*, 933−938.

(74) Chen, B.; Deng, J.; Tong, L.; Yang, W. Optically Active Helical Polyacetylene@silica Hybrid Organic−Inorganic Core/Shell Nanoparticles: Preparation and Application for Enantioselective Crystallization. *Macromolecules* **2010**, *43*, 9613−9619.

(75) Chen, B.; Liu, X.; Xu, C.; Song, C.; Luo, X.; Yang, W.; Deng, J. Aqueous Emulsion Polymerization of Substituted Acetylenes: Effects of Organic Solvent and Analysis of Blue Shifts and Emulsion Polymerization Mechanism. *Macromol. Chem. Phys.* **2012**, *213*, 603−609.

(76) Huber, J.; Mecking, S. Aqueous Poly(arylacetylene) Dispersions. *Macromolecules* **2010**, *43*, 8718−8723.

(77) Liu, G.; Liu, P. Synthesis of Monodispersed Crosslinked Nanoparticles Decorated with Surface Carboxyl Groups via Soapless Emulsion Polymerization. *Colloids Surf., A* **2010**, *354*, 377−381.

(78) Shouldice, G. T. D.; Vandezande, G. A.; Rudin, A. Practical Aspects of the Emulsifier-Free Emulsion Polymerization of Styrene. *Eur. Polym. J.* **1994**, *30*, 179−183.

(79) D'Amato, R.; Medei, L.; Venditti, I.; Russo, M. V.; Falconieri, M. Chemical Synthesis of Polyphenylacetylene Nanospheres with Controlled Dimensions for Photonic Crystals. *Mater. Sci. Eng., C* **2003**, *23*, 861−865.

(80) Reese, C. E.; Guerrero, C. D.; Weissman, J. M.; Lee, K.; Asher, S. A. Synthesis of Highly Charged, Monodisperse Polystyrene Colloidal Particles for the Fabrication of Photonic Crystals. *J. Colloid Interface Sci.* **2000**, *232*, 76−80.

(81) Venditti, I.; D'Amato, R.; Russo, M. V.; Falconieri, M. Synthesis of Conjugated Polymeric Nanobeads for Photonic Bandgap Materials. *Sens. Actuators, B* **2007**, *126*, 35−40.

(82) Pantalei, S.; Zampetti, E.; Macagnano, A.; Bearzotti, A.; Venditti, I.; Russo, M. V. Enhanced Sensory Properties of a Multichannel Quartz Crystal Microbalance Coated with Polymeric Nanobeads. *Sensors* **2007**, *7*, 2920−2928.

(83) Venditti, I.; Fratoddi, I.; Palazzesi, C.; Prosposito, P.; Casalboni, M.; Cametti, C.; Battocchio, C.; Polzonetti, G.; Russo, M. V. Self-Assembled Nanoparticles of Functional Copolymers for Photonic Applications. *J. Colloid Interface Sci.* **2010**, *348*, 424−430.

(84) Fratoddi, I.; Venditti, I.; Cametti, C.; Palocci, C.; Chronopoulou, L.; Marino, M.; Acconcia, F.; Russo, M. V. Functional Polymeric Nanoparticles for Dexamethasone Loading and Reléase. *Colloids Surf., B* **2012**, *93*, 59−66.

(85) Arias, S.; Freire, F.; Quiñoá, E.; Riguera, R. The Leading Role of Cation−π Interactions in Polymer Chemistry: the Control of the Helical Sense in Solution. *Polym. Chem.* **2015**, *6*, 4725−4733.

(86) Freire, F.; Seco, J. M.; Quiñoá, E.; Riguera, R. Helical Polymer−Metal Complexes: The Role of Metal Ions on the Helicity and the Supramolecular Architecture of Poly(phenylacetylene)s. *Adv. Polym. Sci.* **2013**, *262*, 123−140.

(87) Freire, F.; Seco, J. M.; Quiñoá, E.; Riguera, R. Chiral Amplification and Helical-Sense Tuning by Mono- and Divalent Metals on Dynamic Helical Polymers. *Angew. Chem., Int. Ed.* **2011**, *50*, 11692−11696.

(88) Arias, S.; Freire, F.; Quiñoá, E.; Riguera, R. Nanospheres, Nanotubes, Toroids, and Gels with Controlled Macroscopic Chirality. *Angew. Chem., Int. Ed.* **2014**, *53*, 13720−13724.

(89) Freire, F.; Seco, J. M.; Quiñoá, E.; Riguera, R. Nanospheres with Tunable Size and Chirality from Helical Polymer−Metal Complexes. *J. Am. Chem. Soc.* **2012**, *134*, 19374−19383.

(90) Bergueiro, J.; Freire, F.; Wendler, E. P.; Seco, J. M.; Quiñoá, E.; Riguera, R. The ON/OFF Switching by Metal Ions of the "Sergeants and Soldiers" Chiral Amplification Effect on Helical Poly-(phenylacetylene)s. *Chem. Sci.* **2014**, *5*, 2170−2176.

(91) Goto, H.; Zhang, H. Q.; Yashima, E. Chiral Stimuli-Responsive Gels: Helicity Induction in Poly(phenylacetylene) Gels Bearing a Carboxyl Group with Chiral Amines. *J. Am. Chem. Soc.* **2003**, *125*, 2516−2523.

(92) Maeda, K.; Matsushita, Y.; Ezaka, M.; Yashima, E. Layer-by-layer Assembly of Charged Poly(phenylacetylene)s with Induced Macro-molecular Helicity. *Chem. Commun.* **2005**, 4152−4154.

(93) Sakurai, S.; Okoshi, K.; Kumaki, J.; Yashima, E. Two-Dimensional Hierarchical Self-Assembly of One-Handed Helical Polymers on Graphite. *Angew. Chem., Int. Ed.* **2006**, *45*, 1245−1248.

(94) Nishimura, T.; Takatani, K.; Sakurai, S.; Maeda, K.; Yashima, E. A Helical Array of Pendant Fullerenes on an Optically Active Polyphenylacetylene. *Angew. Chem., Int. Ed.* **2002**, *41*, 3602−3604.

(95) Sakurai, S.; Ohira, A.; Suzuki, Y.; Fujito, R.; Nishimura, T.; Kunitake, M.; Yashima, E. Synthesis and Property of Helical poly(phenylacetylene)s Bearing Chiral Ruthenium Complexes and Real Space Imaging of Meso- and Nanoscopic Structures. *J. Polym. Sci., Part A: Polym. Chem.* **2004**, *42*, 4621−4640.

(96) Okoshi, K.; Sakurai, S.; Ohsawa, S.; Kumaki, J.; Yashima, E. Control of Main-Chain Stiffness of a Helical Poly(phenylacetylene) by Switching On and Off the Intramolecular Hydrogen Bonding through Macromolecular Helicity Inversion. *Angew. Chem., Int. Ed.* **2006**, *45*, 8173−8176.

(97) Sakurai, S.; Ohsawa, S.; Nagai, K.; Okoshi, K.; Kumaki, J.; Yashima, E. Two-Dimensional Helix-Bundle Formation of a Dynamic Helical Poly(phenylacetylene) with Achiral Pendant Groups on Graphite. *Angew. Chem., Int. Ed.* **2007**, *46*, 7605−7608.

(98) Ohsawa, S.; Sakurai, S.; Nagai, K.; Banno, M.; Maeda, K.; Kumaki, J.; Yashima, E. Hierarchical Amplification of Macromolecular Helicity of Dynamic Helical Poly(phenylacetylene)s Composed of Chiral and Achiral Phenylacetylenes in Dilute Solution, Liquid Crystal, and Two-Dimensional Crystal. *J. Am. Chem. Soc.* **2011**, *133*, 108−114.

(99) Ohsawa, S.; Sakurai, S.; Nagai, K.; Maeda, K.; Kumaki, J.; Yashima, E. Amplification of Macromolecular Helicity of Dynamic Helical Poly(phenylacetylene)s Bearing Non Racemic Alanine Pendants in Dilute Solution, Liquid Crystal and Two-Dimensional Crystal. *Polym. J.* **2012**, *44*, 42−50.

(100) Okoshi, K.; Sakajiri, K.; Kumaki, J.; Yashima, E. Well-Defined Lyotropic Liquid Crystalline Properties of Rigid-Rod Helical Polyacetylenes. *Macromolecules* **2005**, *38*, 4061−4064.

(101) Percec, V.; Obata, M.; Rudick, J. G.; De, B. B.; Glodde, M.; Bera, T. K.; Magonov, S. N.; Balagurusamy, V. S. K.; Heiney, P. A. Synthesis, Structural Analysis, and Visualization of Poly(2-ethynyl-9-substituted carbazole)s and Poly(3-ethynyl-9-substituted carbazole)s Containing Chiral and Achiral Minidendritic Substituents. *J. Polym. Sci., Part A: Polym. Chem.* **2002**, *40*, 3509−3533.

(102) Percec, V.; Rudick, J. G.; Peterca, M.; Staley, S. R.; Wagner, M.; Obata, M.; Mitchell, C. M.; Cho, W.-D.; Balagurusamy, V. S. K.; Lowe, J. N.; Glodde, M.; Weichold, O.; Chung, K. J.; Ghionni, N.; Magonov, S. N.; Heiney, P. A. Synthesis, Structural Analysis, and Visualization of a Library of Dendronized Polyphenylacetylenes. *Chem. - Eur. J.* **2006**, *12*, 5731−5746.

(103) Percec, V.; Rudick, J. G.; Wagner, M.; Obata, M.; Mitchell, C. M.; Cho, W.-D.; Magonov, S. N. AFM Visualization of Individual and Periodic Assemblies of a Helical Dendronized Polyphenylacetylene on Graphite. *Macromolecules* **2006**, *39*, 7342−7351.

(104) Liu, J.; Lam, J. W. Y.; Tang, B. Z. Synthesis and Functionality of Substituted Polyacetylenes. In *Design and Synthesis of Conjugated Polymers*; Leclerc, M., Morin, J.-F., Eds.; Wiley-VCH: Weinheim, Germany, 2010; pp 1−43.

(105) Lam, J. W. Y.; Kong, X.; Dong, Y.; Cheuk, K. K. L.; Xu, K.; Tang, B. Z. Synthesis and Properties of Liquid Crystalline Polyacetylenes with Different Spacer Lengths and Bridge Orientations. *Macromolecules* **2000**, *33*, 5027−5040.

(106) Kong, X.; Tang, B. Z. Synthesis and Novel Mesomorphic Properties of the Side-Chain Liquid Crystalline Polyacetylenes Containing Phenyl Benzoate Mesogens with Cyano and Methoxy Tails. *Chem. Mater.* **1998**, *10*, 3352−3363.

(107) Koltzenburg, S.; Wolff, D.; Stelzer, F.; Springer, J.; Nuyken, O. Investigation of the Thermal and Morphological Behavior of Liquid-Crystalline Acetylene Homo- and Copolymers. *Macromolecules* **1998**, *31*, 9166−9173.

(108) Rudick, J. G.; Percec, V. Helical Chirality in Dendronized Polyarylacetylenes. *New J. Chem.* **2007**, *31*, 1083−1096.

(109) Tang, B. Z.; Kong, X.; Wan, X.; Feng, X.-D. Synthesis and Properties of Stereoregular Polyacetylenes Containing Cyano Groups, Poly[[4-[[[*n*-[(4′-cyano-4-biphenylyl)- oxy]alkyl]oxy]carbonyl]-phenyl]acetylenes]. *Macromolecules* **1997**, *30*, 5620−5628.

(110) Tang, B. Z.; Kong, X.; Wan, X.; Peng, H.; Lam, W. Y.; Feng, X.-D.; Kwok, H. S. Liquid Crystalline Polyacetylenes: Synthesis and Properties of Poly{*n*-[((4′-cyano-4-biphenylyl)oxy)carbonyl]-1-alkynes}. *Macromolecules* **1998**, *31*, 2419−2432.

(111) Kong, X.; Lam, J. W. Y.; Tang, B. Z. Synthesis, Mesomorphism, Isomerization, and Aromatization of Stereoregular Poly{[4-({[6-({[4′-(heptyl)oxy-4-biphenylyl]carbonyl}oxy)- hexyl]oxy}carbonyl)phenyl]-acetylene}. *Macromolecules* **1999**, *32*, 1722−1730.

(112) Lam, J. W. Y.; Dong, Y.; Cheuk, K. K. L.; Luo, J.; Xie, Z.; Kwok, H. S.; Mo, Z.; Tang, B. Z. Liquid Crystalline and Light Emitting Polyacetylenes: Synthesis and Properties of Biphenyl-Containing Poly(1-alkynes) with Different Functional Bridges and Spacer Lengths. *Macromolecules* **2002**, *35*, 1229−1240.

(113) Lam, J. W. Y.; Luo, J.; Dong, Y.; Cheuk, K. K. L.; Tang, B. Z. Functional Polyacetylenes: Synthesis, Thermal Stability, Liquid Crystallinity, and Light Emission of Polypropiolates. *Macromolecules* **2002**, *35*, 8288−8299.

(114) Ting, C.-H.; Chen, J.-T.; Hsu, C.-S. Synthesis and Thermal and Photoluminescence Properties of Liquid Crystalline Polyacetylenes Containing 4-Alkanyloxyphenyl *trans*-4-Alkylcyclohexanoate Side Groups. *Macromolecules* **2002**, *35*, 1180−1189.

(115) Lam, J. W. Y.; Tang, B. Z. Liquid-Crystalline and Light-Emitting Polyacetylenes. *J. Polym. Sci., Part A: Polym. Chem.* **2003**, *41*, 2607−2629.

(116) Zhang, X. A.; Zhao, H.; Gao, Y.; Tong, J.; Shan, L.; Chen, Y.; Zhang, S.; Qin, A.; Sun, J. Z.; Tang, B. Z. Functional Poly-(phenylacetylene)s Carrying Azobenzene Pendants: Polymer Synthesis, Photoisomerization Behaviors, and Liquid-Crystalline Property. *Polymer* **2011**, *52*, 5290−5301.

(117) San Jose, B. A.; Matsushita, S.; Moroishi, Y.; Akagi, K. Disubstituted Liquid Crystalline Polyacetylene Derivatives That Exhibit Linearly Polarized Blue and Green Emissions. *Macromolecules* **2011**, *44*, 6288−6302.

(118) San Jose, B. A.; Akagi, K. Liquid Crystalline Polyacetylene Derivatives with Advanced Electrical and Optical Properties. *Polym. Chem.* **2013**, *4*, 5144−5161.

(119) Watanabe, K.; Akagi, K. Helically Assembled π-Conjugated Polymers with Circularly Polarized Luminescence. *Sci. Technol. Adv. Mater.* **2014**, *15*, 044203.

(120) Schenning, A. P. H. J.; Fransen, M.; Meijer, E. W. Side-Chain-Functionalized Polyacetylenes, 1. Liquid Crystalline and Stereomutational Properties. *Macromol. Rapid Commun.* **2002**, *23*, 265−270.

(121) Maeda, K.; Takeyama, Y.; Sakajiri, K.; Yashima, E. Nonracemic Dopant-Mediated Hierarchical Amplification of Macromolecular Helicity in a Charged Polyacetylene Leading to a Cholesteric Liquid Crystal in Water. *J. Am. Chem. Soc.* **2004**, *126*, 16284−16285.

(122) Nagai, K.; Sakajiri, K.; Maeda, K.; Okoshi, K.; Sato, T.; Yashima, E. Hierarchical Amplification of Macromolecular Helicity in a Lyotropic Liquid Crystalline Charged Poly(phenylacetylene) by Nonracemic Dopants in Water and Its Helical Structure. *Macromolecules* **2006**, *39*, 5371−5380.

(123) Morimoto, M.; Tamura, K.; Nagai, K.; Yashima, E. Chirality Sensing of Chiral Pyrrolidines and Piperazines with a Liquid Crystalline Dynamic Helical Poly(phenylacetylene) Bearing Ethyl Phosphonate Pendant Groups. *J. Polym. Sci., Part A: Polym. Chem.* **2010**, *48*, 1383−1390.

(124) Fukushima, T.; Kimura, H.; Tsuchihara, K. Color and Chiroptical Control of Poly(phenylacetylene) Films with Chiral Hydroxyl Group. *Macromolecules* **2009**, *42*, 8619−8626.

(125) Okoshi, K.; Kajitani, T.; Nagai, K.; Yashima, E. Uniaxial Orientation of a Rodlike Helical Poly(phenylacetylene) in an Electric Field. *Macromolecules* **2008**, *41*, 258−261.

(126) Mawatari, Y.; Tabata, M.; Sone, T.; Ito, K.; Sadahiro, Y. Origin of Color of π-Conjugated Columnar Polymers. 1. Poly(p-3-methylbutoxy)phenylacetylene Prepared Using a [Rh(norbornadiene)-Cl]₂ Catalyst. *Macromolecules* **2001**, *34*, 3776−3782.

(127) Motoshige, A.; Mawatari, Y.; Motoshige, R.; Yoshida, Y.; Tabata, M. Contracted Helix to Stretched Helix Rearrangement of an Aromatic Polyacetylene Prepared in *n*-Hexane with [Rh-(norbornadiene)Cl]₂-triethylamine Catalyst. *J. Polym. Sci., Part A: Polym. Chem.* **2013**, *51*, 5177−5183.

(128) Motoshige, R.; Mawatari, Y.; Motoshige, A.; Yoshida, Y.; Sasaki, T.; Yoshimizu, H.; Suzuki, T.; Tsujita, Y.; Tabata, M. Mutual Conversion Between Stretched and Contracted Helices Accompanied by a Drastic Change in Color and Spatial Structure of Poly-(phenylacetylene) Prepared with a [Rh(nbd)Cl]₂-amine Catalyst. *J. Polym. Sci., Part A: Polym. Chem.* **2014**, *52*, 752−759.

(129) Percec, V.; Rudick, J. G.; Peterca, M.; Wagner, M.; Obata, M.; Mitchell, C. M.; Cho, W.-D.; Balagurusamy, V. S. K.; Heiney, P. A. Thermoreversible Cis-Cisoidal to Cis-Transoidal Isomerization of Helical Dendronized Polyphenylacetylenes. *J. Am. Chem. Soc.* **2005**, *127*, 15257−15264.

(130) Percec, V.; Peterca, M.; Rudick, J. G.; Aqad, E.; Imam, M. R.; Heiney, P. A. Self-Assembling Phenylpropyl Ether Dendronized Helical Polyphenylacetylenes. *Chem. - Eur. J.* **2007**, *13*, 9572−9581.

(131) Percec, V.; Aqad, E.; Peterca, M.; Rudick, J. G.; Lemon, L.; Ronda, J. C.; De, B. B.; Heiney, P. A.; Meijer, E. W. Steric Communication of Chiral Information Observed in Dendronized Polyacetylenes. *J. Am. Chem. Soc.* **2006**, *128*, 16365−16372.

(132) Percec, V.; Rudick, J. G.; Peterca, M.; Aqad, E.; Imam, M. R.; Heiney, P. A. Synthesis, Structural, and Retrostructural Analysis of Helical Dendronized Poly(1-naphthylacetylene)s. *J. Polym. Sci., Part A: Polym. Chem.* **2007**, *45*, 4974−4987.

(133) Liu, X.-Q.; Wang, J.; Yang, Sh.; Chen, E.-Q. Self-Organized Columnar Phase of Side-Chain Liquid Crystalline Polymers: To Precisely Control the Number of Chains Bundled in a Supramolecular Column. *ACS Macro Lett.* **2014**, *3*, 834−838.

(134) Percec, V.; Rudick, J. G.; Peterca, M.; Heiney, P. A. Nanomechanical Function from Self-Organizable Dendronized Helical Polyphenylacetylenes. *J. Am. Chem. Soc.* **2008**, *130*, 7503−7508.

(135) Rudick, J. G.; Percec, V. Nanomechanical Function Made Possible by Suppressing Structural Transformations of Polyarylacetylenes. *Macromol. Chem. Phys.* **2008**, *209*, 1759−1768.

(136) Rudick, J. Nanomechanical Function Arising from the Complex Architecture of Dendronized Helical Polymers. *Adv. Polym. Sci.* **2013**, *262*, 345−362.

(137) Xu, H.-P.; Xie, B.-Y.; Yuan, W.-Z.; Sun, J.-Z.; Yang, F.; Dong, Y.-Q.; Qin, A.; Zhang, S.; Wang, M.; Tang, B. Z. Hybridization of Thiol-Functionalized Poly(phenylacetylene) with Cadmium Sulfide Nanorods: Improved Miscibility and Enhanced Photoconductivity. *Chem. Commun.* **2007**, 1322−1324.

(138) Xu, H.; Jin, J. K.; Mao, Y.; Sun, J. Z.; Yang, F.; Yuan, W. Z.; Dong, Y.-Q.; Wang, M.; Tang, B. Z. Synthesis of Sulfur-Containing Polyacetylenes and Fabrication of Their Hybrids with ZnO Nanoparticles. *Macromolecules* **2008**, *41*, 3874−3883.

(139) Nishimura, T.; Ohsawa, S.; Maeda, K.; Yashima, E. A Helical Array of Pendant Fullerenes on a Helical Poly(phenylacetylene) Induced by Non-Covalent Chiral Interactions. *Chem. Commun.* **2004**, 646−647.

(140) Nishimura, T.; Tsuchiya, K.; Ohsawa, S.; Maeda, K.; Yashima, E.; Nakamura, Y.; Nishimura, J. Macromolecular Helicity Induction on a Poly(phenylacetylene) with C_2-Symmetric Chiral [60]Fullerene-Bisadducts. *J. Am. Chem. Soc.* **2004**, *126*, 11711−11717.

(141) Tang, B. Z.; Xu, H.; Lam, J. W. Y.; Lee, P. P. S.; Xu, K.; Sun, Q.; Cheuk, K. K. L. C₆₀-Containing Poly(1-phenyl-1-alkynes): Synthesis, Light Emission, and Optical Limiting. *Chem. Mater.* **2000**, *12*, 1446−1455.

(142) Sun, J. Z.; Qin, A.; Tang, B. Z. Functional Polyacetylenes: Hybrids with Carbon Nanotubes. *Polym. Chem.* **2013**, *4*, 211−223.

(143) Tang, B. Z.; Xu, H. Preparation, Alignment, and Optical Properties of Soluble Poly(phenylacetylene)-Wrapped Carbon Nanotubes. *Macromolecules* **1999**, *32*, 2569−2576.

(144) Yuan, W. Z.; Sun, J. Z.; Dong, Y. Q.; Häußler; Yang, M. F.; Xu, H. P.; Qin, A.; Lam, J. W. Y.; Zheng, Q.; Tang, B. Z. Wrapping Carbon Nanotubes in Pyrene-Containing Poly(phenylacetylene) Chains: Solubility, Stability, Light Emission, and Surface Photovoltaic Properties. *Macromolecules* **2006**, *39*, 8011−8020.

(145) Bahun, G. J.; Wang, C.; Adronov, A. Solubilizing Single-Walled Carbon Nanotubes With Pyrene-Functionalized Block Copolymers. *J. Polym. Sci., Part A: Polym. Chem.* **2006**, *44*, 1941−1951.

(146) Yuan, W. Z.; Mao, Y.; Zhao, H.; Sun, J. Z.; Xu, H. P.; Jin, J. K.; Zheng, Q.; Tang, B. Z. Electronic Interactions and Polymer Effect in the Functionalization and Solvation of Carbon Nanotubes by Pyrene- and Ferrocene-Containing Poly(1-alkyne)s. *Macromolecules* **2008**, *41*, 701−707.

(147) Zhao, H.; Yuan, W. Z.; Mei, J.; Tang, L.; Liu, X. Q.; Yan, J. M.; Shen, X. Y.; Sun, J. Z.; Qin, A.; Tang, B. Z. Enhanced Dispersion of Nanotubes in Organic Solvents by Donor−Acceptor Interaction Between Functionalized Poly(phenylacetylene) Chains and Carbon Nanotube Walls. *J. Polym. Sci., Part A: Polym. Chem.* **2009**, *47*, 4995−5005.

(148) Yuan, W. Z.; Sun, J. Z.; Liu, J. Z.; Dong, Y. Q.; Li, Z.; Xu, H. P.; Qin, A.; Häussler, M.; Jin, J. K.; Zheng, Q.; Tang, B. Z. Processable Hybrids of Ferrocene-Containing Poly(phenylacetylene)s and Carbon Nanotubes: Fabrication and Properties. *J. Phys. Chem. B* **2008**, *112*, 8896−8905.

(149) Yuan, W. Z.; Lam, J. W. Y.; Shen, J. Z.; Sun, J. Z.; Mahtab, F.; Zheng, Q.; Tang, B. Z. Functional Polyacetylenes Carrying Mesogenic and Polynuclear Aromatic Pendants: Polymer Synthesis, Hybridization with Carbon Nanotubes, Liquid Crystallinity, Light Emission, and Electrical Conductivity. *Macromolecules* **2009**, *42*, 2523−2531.

(150) Zhao, H.; Yuan, W. Z.; Tang, L.; Sun, J. Z.; Xu, H.; Qin, A.; Mao, Y.; Jin, J. K.; Tang, B. Z. Hybrids of Triphenylamine-Functionalized Polyacetylenes and Multiwalled Carbon Nanotubes: High Solubility, Strong Donor−Acceptor Interaction, and Excellent Photoconductivity. *Macromolecules* **2008**, *41*, 8566−8574.

(151) Yuan, W. Z.; Tang, L.; Zhao, H.; Jin, J. K.; Sun, J. S.; Qin, A.; Xu, H. P.; Liu, J.; Yang, F.; Zheng, Q.; Chen, E.; Tang, B. Z. Direct Polymerization of Highly Polar Acetylene Derivatives and Facile Fabrication of Nanoparticle-Decorated Carbon Nanotubes. *Macromolecules* **2009**, *42*, 52−61.

(152) Yuan, W. Z.; Zhao, H.; Shen, X. Y.; Mahtab, F.; Lam, J. W. Y.; Sun, J. S.; Tang, B. Z. Luminogenic Polyacetylenes and Conjugated Polyelectrolytes: Synthesis, Hybridization with Carbon Nanotubes, Aggregation-Induced Emission, Superamplification in Emission Quenching by Explosives, and Fluorescent Assay for Protein Quantitation. *Macromolecules* **2009**, *42*, 9400−9411.

(153) Wang, X.; Gao, Y.; Zhao, H.; Liu, X.-Q.; Wang, Z.; Qin, A.; Hu, Q.; Sun, J. Z.; Tang, B. Z. Monosaccharide-Functionalized Poly-(phenylacetylenes): *in situ* Polymerization, Hybridization with MWCNTs, and Application in the Reinforcement of Chitosan Rods. *Polym. Chem.* **2014**, *5*, 6216−6224.

(154) Liu, X.-Q.; Li, Y.-L.; Lin, Y.-W.; Yang, S.; Guo, X.-F.; Li, Y.; Yang, J.; Chen, E.-Q. Composites of Functional Poly-(phenylacetylene)s and Single-Walled Carbon Nanotubes: Preparation, Dispersion, and Near Infrared Photoresponsive Properties. *Macromolecules* **2013**, *46*, 8479−8487.

(155) Akai, Y.; Yamamoto, T.; Nagata, Y.; Ohmura, T.; Suginome, M. Enhanced Catalyst Activity and Enantioselectivity with Chirality-Switchable Polymer Ligand PQXphos in Pd-Catalyzed Asymmetric Silaborative Cleavage of meso-Methylenecyclopropanes. *J. Am. Chem. Soc.* **2012**, *134*, 11092−11095.

(156) Suginome, M.; Yamamoto, T.; Nagata, Y.; Yamada, T.; Akai, Y. Catalytic Asymmetric Synthesis Using Chirality-Switchable Helical Polymer as a Chiral Ligand. *Pure Appl. Chem.* **2012**, *84*, 1759−1769.

(157) Iida, H.; Tang, Z.; Yashima, E. Synthesis and Bifunctional Asymmetric Organocatalysis of Helical Poly(phenylacetylene)s Bearing Cinchona Alkaloid Pendants via a Sulfonamide Linkage. *J. Polym. Sci., Part A: Polym. Chem.* **2013**, *51*, 2869−2879.

(158) Tang, Z.; Iida, H.; Hu, H.-Y.; Yashima, E. Remarkable Enhancement of the Enantioselectivity of an Organocatalyzed Asymmetric Henry Reaction Assisted by Helical Poly-(phenylacetylene)s Bearing Cinchona Alkaloid Pendants via an Amide Linkage. *ACS Macro Lett.* **2012**, *1*, 261−265.

(159) Miyake, G. M.; Iida, H.; Hu, H.-Y.; Tang, Z.; Chen, E. Y. -X.; Yashima, E. Synthesis of Helical Poly(phenylacetylene)s Bearing Cinchona Alkaloid Pendants and their Application to Asymmetric Organocatalysis. *J. Polym. Sci., Part A: Polym. Chem.* **2011**, *49*, 5192−5198.

(160) Zhang, D.; Zhang, H.; Song, C.; Yang, W.; Deng, J. Chiral Microspheres Constructed by Helical Substituted Polyacetylene: a New Class of Organocatalyst Toward Asymmetric Catalysis. *Synth. Met.* **2012**, *162*, 1858−1863.

(161) Anger, E.; Iida, H.; Yamaguchi, T.; Hayashi, K.; Kumano, D.; Crassous, J.; Vanthuyne, N.; Roussel, C.; Yashima, E. Synthesis and Chiral Recognition Ability of Helical Polyacetylenes Bearing Helicene Pendants. *Polym. Chem.* **2014**, *5*, 4909−4914.

(162) Shimomura, K.; Ikai, T.; Kanoh, S.; Yashima, E.; Maeda, K. Switchable Enantioseparation Based on Macromolecular Memory of a Helical Polyacetylene in the Solid State. *Nat. Chem.* **2014**, *6*, 429−434.

(163) Naito, Y.; Tang, Z.; Iida, H.; Miyabe, T.; Yashima, E. Poly(phenylacetylene)s Bearing Cinchona Alkaloid Pendants as Chiral Stationary Phases for HPLC. *Chem. Lett.* **2012**, *41*, 809−811.

(164) Cheuk, K. K. L.; Lam, J. W. Y.; Li, B. Sh.; Xie, Y.; Tang, B. Z. Decorating Conjugated Polymer Chains with Naturally Occurring Molecules: Synthesis, Solvatochromism, Chain Helicity, and Biological Activity of Sugar-Containing Poly(phenylacetylene)s. *Macromolecules* **2007**, *40*, 2633−2642.